AN INVESTIGATION INTO THE ROLES OF ATG8 PROTEINS IN AUTOPHAGY INITIATION

A Thesis
SUBMITTED TO THE FACULTY OF THE
UNIVERSITY OF MINNESOTA
BY

Douglas Samuel Grunwald

IN PARTIAL FULFILLMENT OF THE REQUIREMENTS
FOR THE DEGREE OF
DOCTOR OF PHILOSOPHY

Dr. Do-Hyung Kim, Advisor

August 2018

Acknowledgements

I thank my graduate advisor Dr. Do-Hyung Kim. His teachings have played an invaluable role in this study and also in my growth as a researcher. His knowledge, optimism, and patience are virtues that I admire greatly and will always remember.

I also thank all members of the Kim Lab, past and present. I especially thank Ji-Man Park, who has been very generous in sharing his time, ideas, and knowledge, and Daihyun Song and Neil Otto for contributing important experiments to this study.

I would also like to thank all members of my committee. I especially thank Dr. Deborah Ferrington for all her advice and motivating words.

Lastly, I would like to thank my colleagues and fellow graduate students in neighboring labs. I appreciate the assistance that members of the Ervasti Lab have provided with microscopy, the Kyba Lab for their help with cell sorting, and the Bernlohr Lab for their assistant with qRT-PCR and helpful discussions.

For Ashley, Elijah, and Phoebe

Abstract

Autophagy is an intracellular degradation process that occurs in all eukaryotes. Despite being critical for cellular and organismal homeostasis, the mechanism of autophagy remains poorly understood. To address this important question, we aimed to define protein-protein interactions of the Unc-51-like kinase 1 (ULK1) complex, a protein complex critical for transducing stress signals, such as nutrient starvation, to the autophagy machinery. In human cells, the ULK1 complex is composed of ULK1, ATG13, FIP200, and ATG101. Members ULK1, ATG13, and FIP200 were previously shown to bind to ATG8 proteins through their LC3-interacting regions (LIR), however the functional significance of the interaction remains unclear. Human cells express at least six proteins, referred to collectively as ATG8 proteins, which are homologous to the single yeast Atg8 protein. This study reveals that the binding of ATG8 proteins to the ULK1 complex plays an important role in activating ULK1 and initiating autophagy in response to starvation. ATG8 proteins are classified into two subfamilies, the LC3 and GABARAP subfamily. Using human cells depleted of each subfamily, we found that the GABARAP subfamily promotes ULK1 activity whereas the LC3 subfamily suppresses ULK1 activity. Furthermore, we determined that specific GABARAP subfamily members GABARAP and GABARAPL1 have redundant, compensatory functions in promoting ULK1 activity. We found that the LC3 members LC3B and LC3C suppress ULK1 activity and the expression of the GABARAP subfamily of proteins. By disrupting the endogenous ULK1-ATG8 interaction in human cells, we determined that ATG8 binding to ULK1 is important for ULK1 activity, the biogenesis of isolation membranes and autophagosomes, and autophagy activity. We also found that ATG8 binding to ATG13, but not FIP200, is important for ULK1 activity. Together, these results demonstrate that, by binding to ULK1 and ATG13, GABARAP and GABRAPL1 play a key role in ULK1 activation and autophagy initiation.

Table of Contents

List of Figures

List of Tables

List of Abbreviations

ULK1: uncoordinated-51 like autophagy kinase 1

ATG: autophagy-related protein

mTORC1: mechanistic target of rapamycin complex 1

FIP200: FAK (focal adhesion kinase)-interacting protein of 200 kDa

PI3KC3: phosphatidylinositol-3-kinase class-III

WIPI2: WD repeat domain phosphoinositide-interacting protein 2

VPS34: vacuolar protein sorting

TIP60: Tat-interacting protein

TRAF6: TNF receptor-associated factor

CUL3: short for the E3 ubiquitin ligase Cullin-3

HEK293T: human embryonic kidney cell line

HCT116: human colon cancer cell line

HeLa: human cervical cancer cell line

LC3: short for MAP1LC3 (microtubule-associated protein 1A/1B light chain 3)

GBRP: GABARAP (gamma-aminobutyric acid receptor-associated protein)

BECN1: BECLIN 1

TUB: TUBULIN

DSP: dithiobis(succinimidyl propionate)

BAFA1: bafilomycin A1

EBSS: Earle's balanced salt solution

CRISPR: clustered regularly interspaced short palindromic repeats

Cas9: CRISPR-associated protein 9

TALEN: Transcription Activator-Like Effector Nuclease

WB: western blotting

IP: immunoprecipitation

LIR: LC3-interacting region

WT: wild type

KO: knock out

CHAPTER 1

INTRODUCTION

1.1. An overview of autophagy

Autophagy is an intracellular degradation process that is critical for maintaining homeostasis in all eukaryotic organisms. Autophagy is activated when cells are deprived of nutrients and energy. Intracellular proteins and lipids are broken down by autophagy into amino acids and fatty acids, which cells then utilize to make energy. In addition to a mechanism to survive starvation, autophagy functions as a quality control mechanism, ridding cells of harmful factors such as protein aggregates, pathogens, lipid droplets, damaged mitochondria and other organelles [1–8]. As these cellular insults are contributing factors to many human diseases [9–12], and many cancer cells utilize autophagy to avoid cell death, to grow, and to metastasize [13–20], activating or inhibiting autophagy could be of great therapeutic benefit. However, if we wish to exploit autophagy for therapeutic purposes, we must first improve our understanding of the mechanism of autophagy and how autophagy is initiated. My thesis is an investigation into the molecular details of how autophagy is initiated.

1.2. The autophagy process

Autophagy (also known as macroautophagy) is a process wherein intracellular constituents are targeted to a specialized membrane structure for degradation by the lysosome (**Figure 1**). During autophagy, a cup-shaped structure called the isolation membrane forms and elongates, engulfing cytoplasmic content such as proteins, lipids, and nucleic acids [21]. The membrane closes on itself to form a double-membrane autophagosome. Upon fusion with a lysosome, the inner membrane of the autophagosome and its sequestered contents are degraded by lysosomal hydrolases,

FIGURE 1

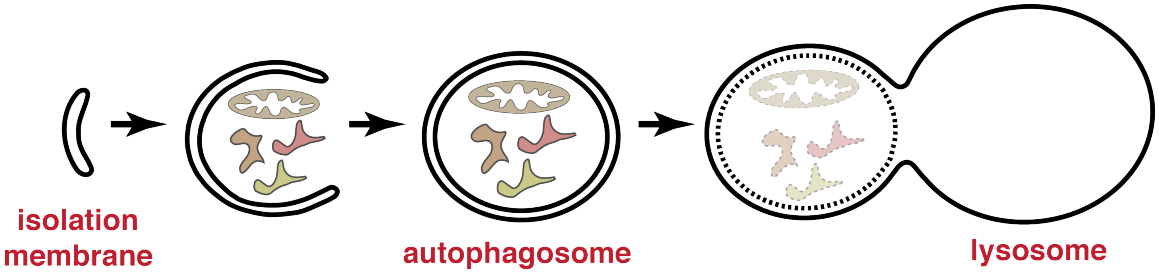

Figure 1. Schematic of the autophagy process. During autophagy a structure called the isolation membrane forms. The endoplasmic reticulum is considered the major membrane contributor to the isolation membrane, although the Golgi apparatus, mitochondria, and plasma membrane have also been described as membrane sources [22–24]. The isolation membrane elongates and then closes to form a double-membrane autophagosome. After fusing with a lysosome, the innermembrane of the autophosome and its captured cytosolic contents are degraded by lysosomal hydrolases.

thereby supplying the cell with amino acids and fatty acids that can be used to generate energy or for anabolic processes to cope with stress.

Autophagy was first described in mammalian cells in the 1960s [25]. Three decades later, the first autophagy-related genes (ATG) essential for autophagy in yeast were identified [26,27]. Many homologous genes have since been identified in humans, and many advances have been made in defining their roles in autophagy. Despite our recent progress in understanding the process, many of the molecular details of autophagy remain elusive. My research has focused on understanding the mechanism for how autophagy is initiated. In this chapter I will summarize the current knowledge on the steps of the mammalian autophagy pathway, with an emphasis on autophagy initiation by the ULK1 complex, the focus of this thesis.

1.3. The initiation of autophagy

Autophagy is initiated when cells are starved for nutrients such as amino acids, growth factors, glucose, or oxygen [28]. The initiation of autophagy depends on the activation of Uncoordinated-51-like kinase 1 (ULK1), a serine/threonine protein kinase that forms a stable protein complex by interacting with ATG13, FAK interacting protein of 200 kDa (FIP200), and ATG101 [29–36]. Mechanistic target of rapamycin complex 1 (mTORC1) plays a major role in regulating autophagy by relaying nutrient signals to the ULK1 complex. Under nutrient-enriched conditions, mTORC1 is active and phosphorylates members of the ULK1 complex to suppress ULK1 and autophagy initiation [33]. Nutrient starvation, or mTORC1 inhibition, releases the suppressive phosphorylation and the ULK1 complex is rapidly dephosphorylated [37], thereby activating ULK1. When active, ULK1 phosphorylates itself, FIP200, and ATG13 and translocates to the endoplasmic reticulum (ER) to facilitate autophagosome nucleation sites [38,39] (**Figure 2**). Several

ULK1-mediated phosphorylations of FIP200 and ATG101 have been identified, however the functions of these phosphorylations are unknown [40].

1.4. Regulation of the ULK1 complex

ULK1 is regulated via phosphorylation by AMPK (AMP-activated protein kinase) and mTORC1. AMPK–mediated phosphorylation of ULK1 is thought to promote ULK1 activity, whereas mTORC1-mediated phosphorylations of ULK1 and its binding partner ATG13 suppress ULK1 activity [41–44]. However, the exact sites of phosphorylation mediated by mTORC1 and AMPK that are responsible for modulating ULK1 activity need to be clarified. In addition to regulating ULK1 directly through phosphorylations, AMPK regulates ULK1 indirectly by phosphorylating and suppressing mTORC1 [45]. ULK1 is also regulated by serum starvation through the GSK3/TIP60 pathway. Glycogen synthase kinase 3 (GSK3) is activated by serum starvation and phosphorylates the acetyltransferase TIP60. Acetylation of ULK1 by TIP60 positively regulates ULK1 activity and autophagy [46].

ULK1 is also regulated by ubiquitination, which depending on the type of ubiquitination, can either promote or suppress ULK1. When mTORC1 is suppressed, the ubiquitin ligase TRAF6 associates with ULK1 and mediates its K63-ubiquitination, which promotes ULK1 stability and activity [47]. This adds another layer of mTORC1-dependent regulation of ULK1 and autophagy. Conversely, ubiquitination of ULK1 can also lead to its degradation by the proteasome. Prolonged starvation leads to ULK1 autophosphorylation at Ser1042 and Thr1046, which directs ULK1 to interact with the ubiquitin ligase CUL3-KLHL20. Subsequent Lys48-ubiquitination of ULK1 by CUL3 results in ULK1 degradation, and is considered to be a mechanism to downregulate ULK1 and terminate autophagy during prolonged starvation [48].

FIGURE 2

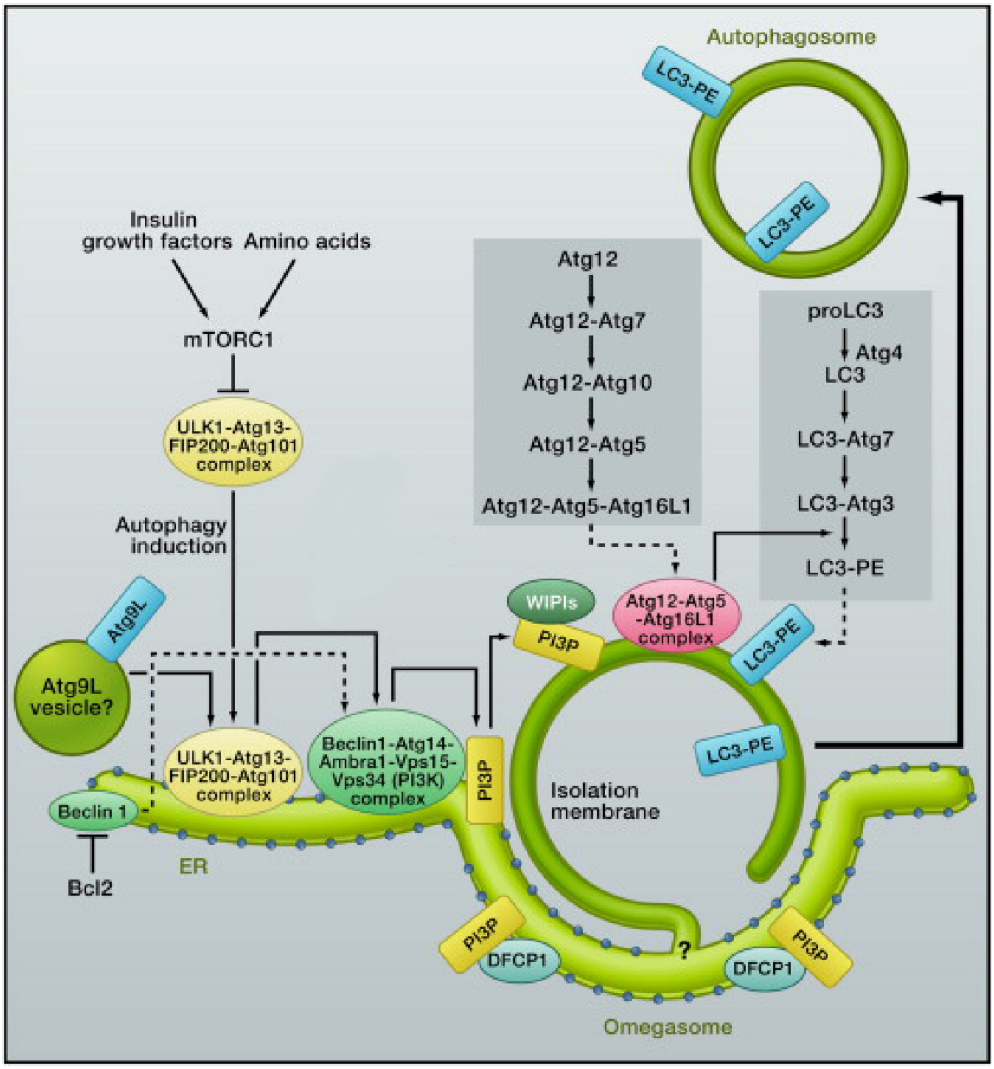
Autophagosome
LC3-PE
LC3-PE
Insulin
growth factors
Amino acids
mTORC1
ULK1-Atg13-
FIP200-Atg101
complex
Autophagy
induction
Atg12
Atg12-Atg7
Atg12-Atg10
Atg12-Atg5
Atg12-Atg5-Atg16L1
proLC3
Atg4
LC3
LC3-Atg7
LC3-Atg3
LC3-PE
WIPIs
PI3P
Atg12-Atg5
-Atg16L1
complex
LC3-PE
Atg9L
Atg9L
vesicle?
ULK1-Atg13-
FIP200-Atg101
complex
Beclin1-Atg14-
Ambra1-Vps15-
Vps34 (PI3K)
complex
PI3P
LC3-PE
Isolation
membrane
Beclin 1
ER
Bcl2
PI3P
DFCP1
?
DFCP1
PI3P
Omegasome

Figure 2. Key mediators and steps of the autophagy process. During nutrient deprivation, when mTORC1 activity is low, the ULK1 complex is activated and translocates to the endoplasmic reticulum (ER). ULK1 phosphorylates the VPS34 (PI3K) complex, thereby activating the lipid kinase VPS34. VPS34 phosphorylates phosphatidylinositol to make phosphatidylinositol 3-phosphate (PI3P). By directly binding PI3P, WIPI and DFCP1 are recruited to membrane and act to recruit autophagy proteins such as the ATG12-ATG5-ATG16L1 complex. ATG4, ATG7, and ATG3 function along with the ATG12-ATG5-ATG16L1 complex to conjugate ATG8 (shown here as LC3) with phosphatidylethanolamine (PE). Growth of the membrane requires PE-conjugated ATG8 as well as ATG9. ATG9 is thought to contribute to the growth of the isolation membrane by mediating the recruitment of small vesicles. PE-conjugated ATG8 also functions in closure of the autophagosome and its subsequent fusion with lysosomes. *Figure adapted from* [49].

1.5. Nucleation of autophagosomes

The activation of phosphatidylinositol-3-kinase class-III (PI3KC3) complex 1 and its translocation to the ER are positively regulated by ULK1 activity and are necessary events for the nucleation of autophagosomes [38,50,51]. PI3KC3 complex 1 is comprised of the lipid kinase VPS34 (vacuolar protein sorting 34), BECLIN 1, ATG14, and VPS15 [52–55]. Under nutrient-enriched conditions, when autophagy activity is low, the PI3KC3 complex is anchored to the cytoskeleton by activating molecule in Beclin 1-regulated autophagy protein 1 (AMBRA1). Upon starvation, ULK1 phosphorylates AMBRA1, thereby promoting the translocation of the PI3KC3 complex from the cytoskeleton to the ER [56]. ULK1 also phosphorylates PI3KC3 members ATG14 and BECLIN 1 at defined residues to enhance the activity of PI3KC3 [57–59] (**Figure 3**). The function of PI3KC3 is to phosphorylate phosphatidylinositol (PI) to generate pools of phosphatidylinositol 3-phosphate (PI3P), marking autophagosome nucleation sites at the ER [60]. Sites enriched for PI3P act to recruit the PI3P-binding proteins WIPI2 (WD repeat domain phosphoinositide-interacting protein 2) and DFCP1 (double FYVE containing protein 1) [61]. WIPI2 and DFCP1 recruit downstream autophagy effectors that are crucial for autophagosome membrane formation and elongation, discussed below.

FIGURE 3

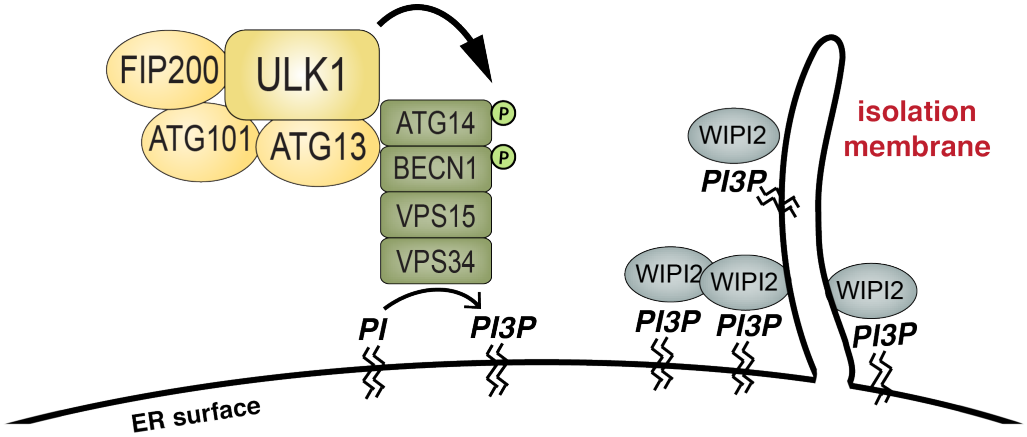

Figure 3. The ULK1 complex activates the PI3KC3 complex 1 via phosphorylation. The ULK1 complex is shown in yellow and the PI3KC3 complex is shown in green. During conditions that favor autophagy, ULK1 is active and phosphorylates PI3KC3 members ATG14 and BECLIN-1 at defined residues [57–59] (depicted as (P)). These phosphorylations depend on the ATG13-ATG14 interaction and enhance the lipid kinase activity of VPS34, and therefore the conversion of PI to PI3P. The PI3P produced by VPS34 is critical for WIPI2 recruitment to the ER and for the biogenesis of the isolation membrane.

1.6. Elongation of the isolation membrane

A crucial step for elongation of the isolation membrane is the covalent linkage of ATG8 proteins with phosphatidylethanolamine (PE), which involves two ubiquitin-like conjugation systems [62,63]. ATG8 shares structural homology with ubiquitin and is cleaved at its C-terminus by the protease ATG4 [64–67]. Cleaved ATG8 is activated via its covalent linkage to the E1-like enzyme ATG7. ATG8 is then transferred to the E2-like enzyme ATG3. Covalent binding of ATG8 to the head group of PE is facilitated by the E3-like enzyme ATG12-ATG5-Atg16L1, a complex formed through a parallel conjugation system [68–70] (**Figure 2 and 4A**). Conjugation of ATG8 with PE is essential for ATG8 localization and for its role in isolation membrane curvature, growth, and fusion [71–73]. However, the exact mechanism for how ATG8 mediates membrane growth and autophagosome-lysosome fusion is unclear. Through its direct interaction with ATG16L1, WIPI2 recruits the ATG12-5-16L1 complex to the nucleation site [74], linking ATG8 conjugation to the isolation membrane [75]. FIP200, by directly interacting with ATG16L1, was also shown to be important for recruiting the ATG12-5-16L1 complex to the isolation membrane [76].

In addition to its role in autophagy initiation, ULK1 regulates ATG9 trafficking during autophagy (**Figure 2**). ATG9 has a transmembrane domain and is the only known integral membrane autophagy protein. During autophagy, vesicles harboring ATG9 are shuttled from the *trans*-Golgi network, plasma membrane, and endosomes to autophagosome nucleation sites, thereby supplying lipids to the growing isolation membrane [77–80]. ATG9 trafficking to the isolation membrane requires phosphorylation by the protein kinase SRC (SRC proto-oncogene, non-receptor tyrosine kinase) and ULK1 [81–83].

FIGURE 4

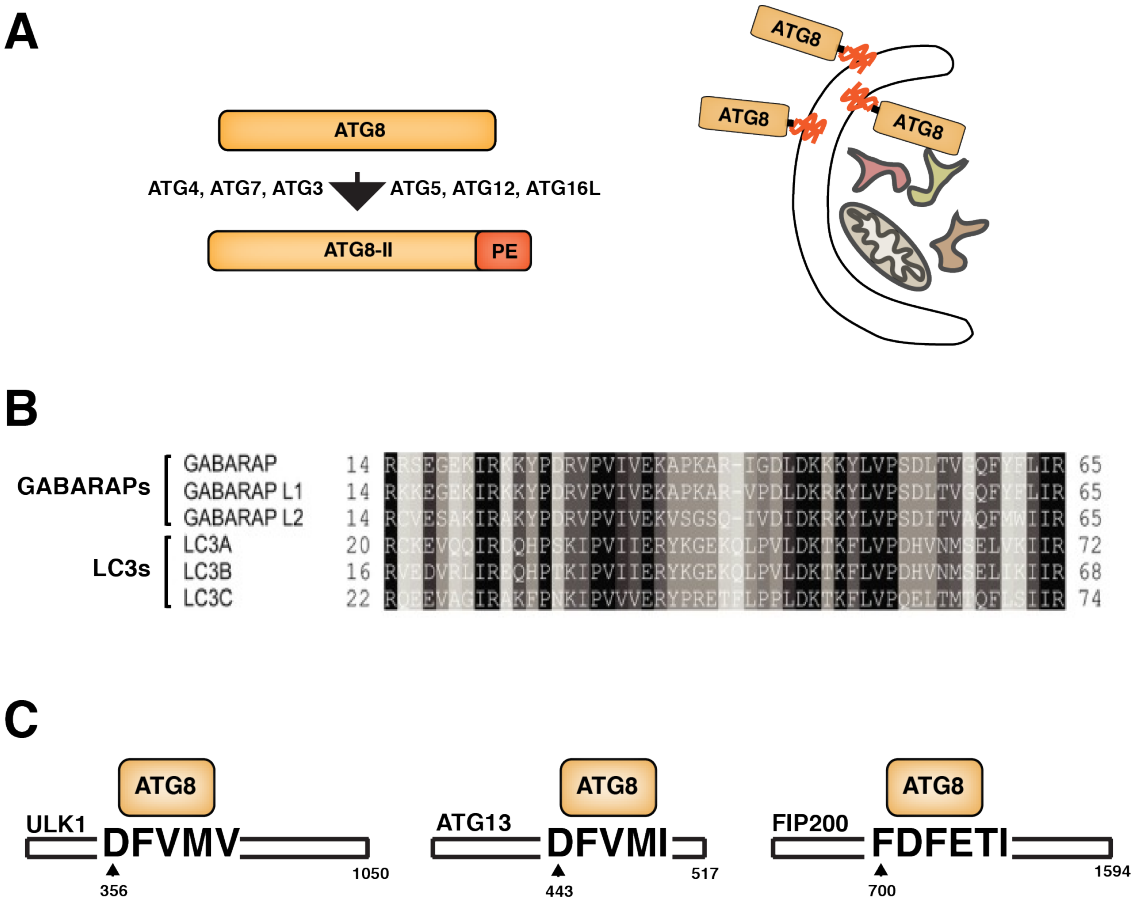

Figure 4. ATG8 proteins and their connection to the ULK1 complex. (A) The PE conjugation of ATG8 is similar to that of ubiquitin conjugation and involves the indicated ATG proteins. PE conjugation tethers ATG8 to inner and outer surfaces of the autophagosomal membrane, where it functions in growth, closure, and fusion of the autophagosome **(B)** The six human ATG8 proteins are divided into two subfamilies based on primary sequence identity, the GABARAP and LC3 subfamilies. Dark shades represent residues with low variability and light shades represent residues with high variability (*Image adapted from* [84]). **(C)** ULK1 complex members ULK1, ATG13, and FIP200 physically interact with ATG8 proteins through their LIR (LC3-interacting region), represented in bold font.

1.7. Human ATG8 proteins and their role in autophagosome growth, closure and fusion with lysosomes

Human cells express at least six proteins, referred to collectively as ATG8 proteins (or simply ATG8s), which are homologous to the single yeast Atg8 protein. Human ATG8 proteins, based on their primary sequence similarity, are classified into one of two subfamilies; the LC3 (microtubule-associated protein 1 light chain 3) subfamily consisting of LC3A, LC3B, and LC3C (referred to collectively as LC3 proteins or LC3s); the GABARAP (GABA type A receptor associated protein) subfamily consisting of GABARAP, GABARAPL1, and GABARAPL2 (referred to collectively as GABARAP proteins or GABARAPs) [85] (**Figure 4B**). All ATG8 proteins contain an ubiquitin-like core composed of β-strands with hydrophobic pockets at their C-termini and a series of α-helices at their N-termini [86]. The N-terminal α-helices of the LC3s are basic, whereas the terminal α-helices of the GABARAPs are acidic or neutral [64]. The divergent N-terminal region of the ATG8s has been speculated to be important for their specific functions.

Each LC3 and GABARAP protein can be conjugated with PE, however they do not necessarily co-localize at the same membrane structure [87,88], suggesting that individual ATG8 proteins might have specific roles. Indeed, the two subfamilies have been suggested to regulate different steps in the autophagy process. The LC3 subfamily appears to function in elongation of the isolation membrane, whereas the GABARAP subfamily is required for closure of the autophagosome and fusion to the lysosome [89–93]. Remarkably, several recent studies have brought the role of LC3 proteins in autophagy into question, suggesting that LC3 proteins are dispensable for autophagy altogether, or are at least less important than the GABARAP subfamily [94,95].

In addition to their role in autophagosome growth, closure, and fusion with lysosomes, ATG8 proteins act as receptors to selectively target cargo to autophagosomes. Certain

cargo that contains the LIR (LC3-interacting region) can directly interact with ATG8 proteins, and thus, is targeted to the autophagosome for degradation [96]. The LIR is defined as (W/F/Y)XX(L/I/V) where X can be any amino acid. Adaptor proteins such as SQSTM1 (p62) and NBR1 contain the LIR and ubiquitin-binding domain, enabling them to bind both ATG8 proteins and ubiquitin simultaneously [97,98]. Through this dual binding, SQSTM1 and NBR1 target ubiquitinated cargo such as protein aggregates for degradation by autophagy [99–101]. ATG8 proteins also target mitochondria for degradation through their interaction with NIX, a LIR-containing adaptor protein that resides at the surface of mitochondria [102].

1.8. Cross-talk between the ULK1 complex and ATG8 proteins

ULK1 complex members ULK1, ATG13, and FIP200 were each found to have LIRs, enabling them to physically interact with ATG8 proteins, however the LIR does not appear to mediate degradation of the ULK1 complex [103–105] (**Figure 4C**). This discovery indicates a potential crosstalk between the autophagy initiation complex and ATG8 proteins. The LIR of ULK1 was found to be important for ULK1 to associate with autophagosomes, implying that the ULK1-ATG8 interaction might play a role in autophagy [103]. A recent study has suggested that GABARAP binding to ULK1 is important for a specific ULK1-mediated phosphorylation of ATG13 [106], a phosphorylation that was previously shown to be important for degradation of mitochondria by autophagy [107]. Although this finding indicates that GABARAP binding to ULK1 might have a role in the selective degradation of mitochondria through autophagy, it remains unknown if the ULK1-ATG8 interaction plays a role in non-selective autophagy. Furthermore, the function of ATG8 binding to ATG13 and FIP200 remains unknown.

1.9. Objectives

The overall goal of my study was to better understand how the initiation of autophagy is regulated through the ULK1 complex. To address this important question, we aimed to define the interaction between the ATG8 proteins and the ULK1 complex. Considering that ATG8 proteins bind to the ULK1 complex, the complex that drives autophagy initiation, **the central hypothesis of my study is that specific ATG8 proteins play a role in initiating autophagy by binding to the ULK1 complex**.

In the first part of my study, I did a comprehensive analysis of the interaction between each of the six ATG8 proteins and each LIR-containing member of the ULK1 complex. Here, the goal was to gain insight into which ATG8 proteins might be regulating the ULK1 complex, based on their binding affinities. For additional insight into the mechanism for how ULK1 is regulated to mediate autophagy, I sought to determine whether the interaction was regulated by conditions that enhance autophagy. In the second part of my study I aimed to define the role of specific ATG8 proteins in autophagy initiation. The final objective was to define the function of ATG8 binding to each member of the ULK1 complex.

CHAPTER 2

THE INTERACTION BETWEEN ATG8 PROTEINS AND THE ULK1 COMPLEX

To understand how the ULK1 complex mediates autophagy, we first aimed to define protein-protein interactions of the ULK1 complex. As mentioned in Chapter 1, members of the ULK1 complex interact with ATG8 proteins [103–105], however, the interactions have not been well defined, especially in a biologically relevant context. In this chapter, we sought to define the interaction between members of the ULK1 complex and ATG8 proteins. Briefly, we observed that, when comparing the two subfamilies, GABARAP proteins have a greater affinity for the ULK1 complex. When comparing members of the ULK1 complex individually, we found that ATG13 interacted with the three GABARAP proteins and LC3C, whereas ULK1 only interacted with the three GABARAP proteins. Interestingly, we did not observe interaction between any of the six ATG8s and FIP200, indicating that ATG8s bind to the ULK1 complex through their interaction with ULK1 and/or ATG13. To gain insight into the function of the ATG8-ULK1 complex interaction, we investigated whether the interaction is regulated by autophagy induction. We found that PE conjugation of GABARAP proteins is important for their binding to ULK1, however nutrient starvation did not appear to affect the interaction. Lastly, we found that the interaction between ULK1 and ATG13 does not require their binding to any ATG8.

2.1. The ULK1 complex differentially binds to ATG8 proteins

Although previous studies have shown that ATG8 proteins bind to members of ULK1 complex *in vitro*, the studies have not demonstrated whether the ULK1 complex, expressed endogenously from human cells, binds to ATG8 proteins. To analyze which ATG8 protein(s) bind to the endogenous ULK1 complex, individual MYC-tagged ATG8 proteins were transiently expressed in HEK293T cells and MYC immunoprecipitates

were isolated. HEK293T is a human embryonic kidney cell line used for its high transfection efficiency [108]. Among the six ATG8 proteins tested, GABARAP and GABARAPL1 were most efficient at co-immunoprecipitating ULK1, ATG13, and FIP200 (**Figure 5**). GABARAPL2 and LC3C co-immunoprecipitated with ULK1 complex members to a lesser degree, while LC3A and LC3B failed to co-immunoprecipitate with ULK1 complex members at a level greater than that of the negative control (empty). These differing binding affinities suggest that certain ATG8 proteins preferentially interact with the ULK1 complex, indicating that specific ATG8 proteins might play a role in regulating the ULK1 complex. Comparing the relative amounts of immunoprecipitated ATG8 proteins, GABARAPL1 appears to have the greatest binding affinity for the ULK1 complex.

To test whether the LIR-containing ULK1 complex members each share a similar affinity for each ATG8, HA-tagged ULK1, FIP200, or ATG13 were co-expressed with individual MYC-tagged ATG8 proteins in HEK293T cells. MYC immunoprecipitates were isolated and the amounts of co-immunoprecipitated HA-tagged ULK1, FIP200, or ATG13 were assessed. HA-ULK1 co-immunoprecipitated with GABARAP, GABARAPL1, and to a lesser degree with GABARAPL2, but not with any LC3 protein at a level greater than that of the negative control (empty) (**Figure 6A**). This result suggests that ULK1 has a strong binding preference for the GABARAP subfamily of ATG8 proteins, which corroborates a previous study [104]. Consistent with the result in Figure 5, GABARAPL1 showed the greatest affinity for ULK1 when comparing the amounts of total ATG8 protein isolated in the MYC immunoprecipitates.

FIGURE 5

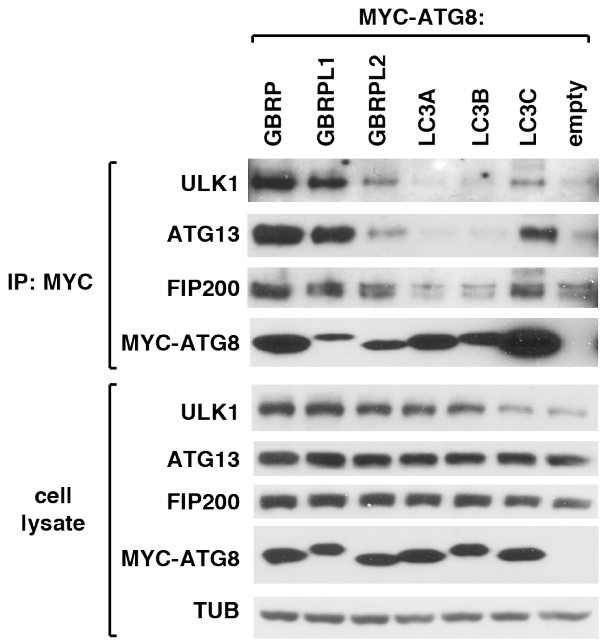

Figure 5. GABARAPs and LC3s interact with endogenous ULK1 complex with differential binding affinities. GABARAP, GABARAPL1, GABARAPL2 and LC3C, but not LC3A or LC3B, interact with the ULK1 complex. MYC-tagged ATG8 proteins were transiently expressed in HEK293T cells and immunoprecipitated with anti-MYC antibody. Endogenous ULK1, ATG13, and FIP200 that were co-immunoprecipitated with MYC-ATG8 were analyzed by western blotting (WB) using the indicated antibodies. TUBULIN (TUB) was assessed for the loading control.

FIGURE 6

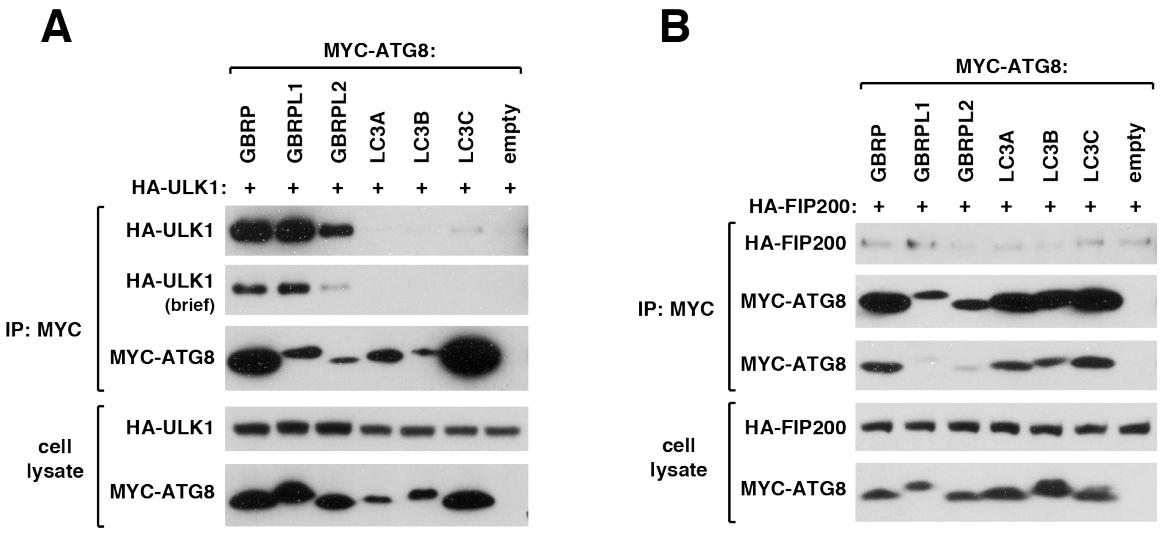

Figure 6. ULK1 interacts with GABARAPs but not LC3s. (A) ULK1 interacts with GABARAP, GABARAPL1, and GABARAPL2. MYC-tagged ATG8 proteins were transiently co-expressed with HA-ULK1 in HEK293T cells. MYC-ATG8 proteins were immunoprecipitated with anti-MYC antibody and co-immunoprecipitated HA-ULK1 was assessed by WB. **(B)** FIP200 does not interact with any ATG8 proteins. The same procedure as described in (A) was followed, except HA-FIP200 was co-expressed instead of HA-ULK1.

HA-FIP200 did not co-immunoprecipitate with any ATG8 protein at a level greater than that of the negative control (**Figure 6B**). Although *in vitro* translated human FIP200 was shown to interact with purified GABARAP *in vitro* [104], this result from our study suggests that human FIP200 expressed in a cellular context might not interact with any of the six ATG8 proteins.

HA-ATG13 co-immunoprecipitated with all three GABARAPs, LC3C, and to a lesser degree with LC3A (**Figure 7A**). Since ATG13 is constitutively bound to ULK1 in human cells [34], it is possible that ATG13 does not bind to ATG8 proteins directly, but rather indirectly, through its interaction with ULK1. To test whether ATG13 binding to ATG8 proteins requires ATG13 to interact with ULK1, we tested whether a C-terminal deletion mutant of ATG13, unable to bind ULK1, can interact with ATG8 proteins. Full length ATG13 (1-517) and the C-terminal deletion mutant of ATG13 (1-510) were co-immunoprecipitated with HA-GABARAP at comparable levels (**Figure 7B**). The ATG13 fragment that excludes its LIR (1-440) and the LIR mutant of ATG13 (**Figure 4C**) were not co-immunoprecipitated with HA-GABARAP, showing that the LIR-sufficient ATG13 that was co-immunoprecipitated is specific. Indeed, the ULK1 binding-deficient mutant of ATG13 is expressed and was able to interact with FIP200, but not ULK1 (**Figure 7C**). This result suggests that ATG13, expressed from cells, does not require its interaction with ULK1 to bind to ATG8, and therefore, likely interacts with ATG8 directly.

FIGURE 7

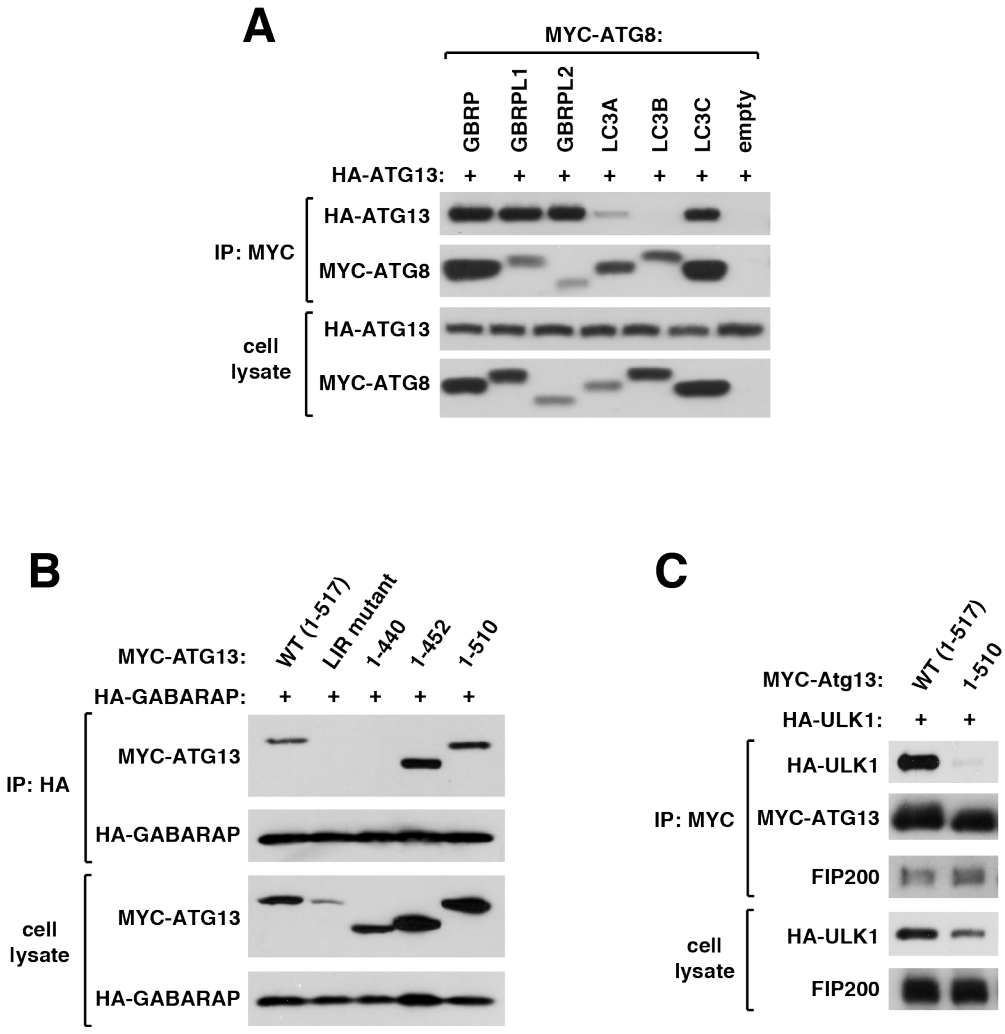
A
MYC-ATG8:
GBRP
GBRPL1
GBRPL2
LC3A
LC3B
LC3C
empty
HA-ATG13: + + + + + + +
IP: MYC
HA-ATG13
MYC-ATG8
cell lysate
HA-ATG13
MYC-ATG8
B
MYC-ATG13:
WT (1-517)
LIR mutant
1-440
1-452
1-510
HA-GABARAP: + + + + +
IP: HA
MYC-ATG13
HA-GABARAP
cell lysate
MYC-ATG13
HA-GABARAP
C
MYC-Atg13:
WT (1-517)
1-510
HA-ULK1: + +
IP: MYC
HA-ULK1
MYC-ATG13
FIP200
cell lysate
HA-ULK1
FIP200

Figure 7. ATG13 interacts with GABARAPs and LC3C. (A) ATG13 interacts with GABARAP, GABARAPL1, GABARAPL2, and LC3C. The indicated MYC-tagged ATG8 proteins were co-expressed with HA-tagged ATG13 in HEK293T cells. MYC-ATG8 proteins were immunoprecipitated with anti-MYC antibody. The amounts of co-immunoprecipitated HA-tagged ATG13 were assessed by WB. **(B)** The ATG13-GABARAP interaction does not depend on ATG13 binding to ULK1. HA-GABARAP was transiently co-expressed with MYC-tagged ATG13 wild type (WT), LIR mutant, or C-terminal deletion fragments of ATG13 (1-440, 1-452, 1-510) in HEK293T cells. Fragment 1-440 excludes the LIR and ULK1 binding region (Figure 4C). Fragments 1-452 and 1-510 include the LIR but exclude the ULK1 binding region. HA-GABARAP was immunoprecipitated using anti-HA antibody and co-immunoprecipitated MYC-tagged ATG13 variants were detected by WB using anti-MYC antibody. **(C)** Verification that ATG13 fragment 1-510 does not bind to ULK1. HA-ULK1 was transiently co-expressed with MYC-ATG13 WT or fragment 1-510 in HEK293T cells. MYC-ATG13 variants were immunoprecipitated with anti-MYC antibody and co-immunoprecipitated HA-ULK1 was assessed by WB. Co-immunoprecipitated endogenous FIP200 was detected as a control to indicate that, other than deficient ULK1 binding, ATG13 1-510 is folded and functional.

2.2. Phospholipid conjugation of GABARAP regulates its binding affinity for ULK1

We suspected that lipid conjugation of GABARAP proteins with phosphatidylethanolamine (PE) might regulate their interaction with the ULK1 complex. To test this possibility, we depleted ATG7, a protein required for the PE conjugation of ATG8 proteins [109], in HEK293T cells using the CRISPR-Cas9 gene editing technique and assessed the co-immunoprecipitation of recombinant GABARAPs and endogenous ULK1. GABARAP and GABARAPL1 were tested because of their high affinity for the ULK1 complex. In the absence of ATG7, the co-immunoprecipitation of the GABARAPs and ULK1 was reduced (**Figure 8**). This result indicates that PE conjugation of the GABARAPs positively regulates their binding affinity for ULK1.

2.3. GABARAP proteins interact with the ULK1 complex independent of nutrient condition

When nutrients are abundant, a condition unfavorable for autophagy, ULK1 and ATG13 are hyper-phosphorylated by mTORC1 [33]. Upon nutrient starvation, ULK1 and ATG13 are dephosphorylated overall. Thus, in addition to PE conjugation of ATG8 proteins, nutrient condition and the phosphorylation status of ULK1 and ATG13 might serve as another mechanism to regulate the interaction between the ATG8 proteins and the ULK1 complex.

To test whether nutrient starvation regulates the binding of ATG8 proteins to the ULK1 complex, HEK293T cells transiently expressing MYC-tagged ATG8 proteins were cultured in full medium or starved for 2 h in EBSS (Earle's Balanced Salt Solution), a medium depleted of amino acids and growth factors that is commonly used to induce autophagy. MYC-immunoprecipitates were isolated and amount of co-immunoprecipitated ULK1 complex was assessed.

FIGURE 8

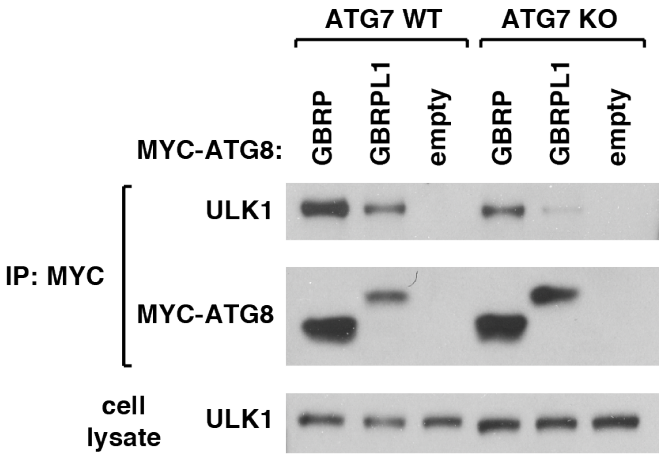

Figure 8. ATG7 positively regulates the binding of GABARAP and GABARAPL1 to ULK1. MYC-GABARAP or MYC-GABARAPL1 were transiently expressed in ATG7 wild type (WT) or ATG7-depleted (KO) HEK293T cells. MYC-tagged GABARAPs were isolated by immunoprecipitation using anti-MYC antibody and amount of co-immunoprecipitated endogenous ULK1 was assessed by WB. Confirmation of ATG7 deficiency in the KO is shown in Figure 12B.

ULK1 complex members were co-immunoprecipitated with GABARAP and GABARAPL2 at similar levels in full medium (fed) versus EBSS (starved), indicating that the interaction of GABARAP and GABARAPL2 with the ULK1 complex is not regulated by starvation and might be constitutive (**Figure 9A**). The co-immunoprecipitation of ULK1 and ATG13 with GABARAPL1 was marginally greater with EBSS versus full medium, suggesting that the binding of GABARAPL1 to the ULK1 complex might be enhanced during conditions that favor autophagy (**Figure 9A**). Interestingly, the co-immunoprecipitation of the ULK1 complex with LC3C was greatly enhanced with EBSS versus full medium, suggesting that the binding of LC3C to the ULK1 complex might be enhanced during autophagy (**Figure 9B**). Consistent with the results from Figure 5, interaction with LC3A and LC3B was not detected. Together these results suggest that the binding of GABARAP proteins to the ULK1 complex is, for the most part, independent of nutrient status, while LC3C binding to the ULK1 complex is positively regulated by starvation.

FIGURE 9

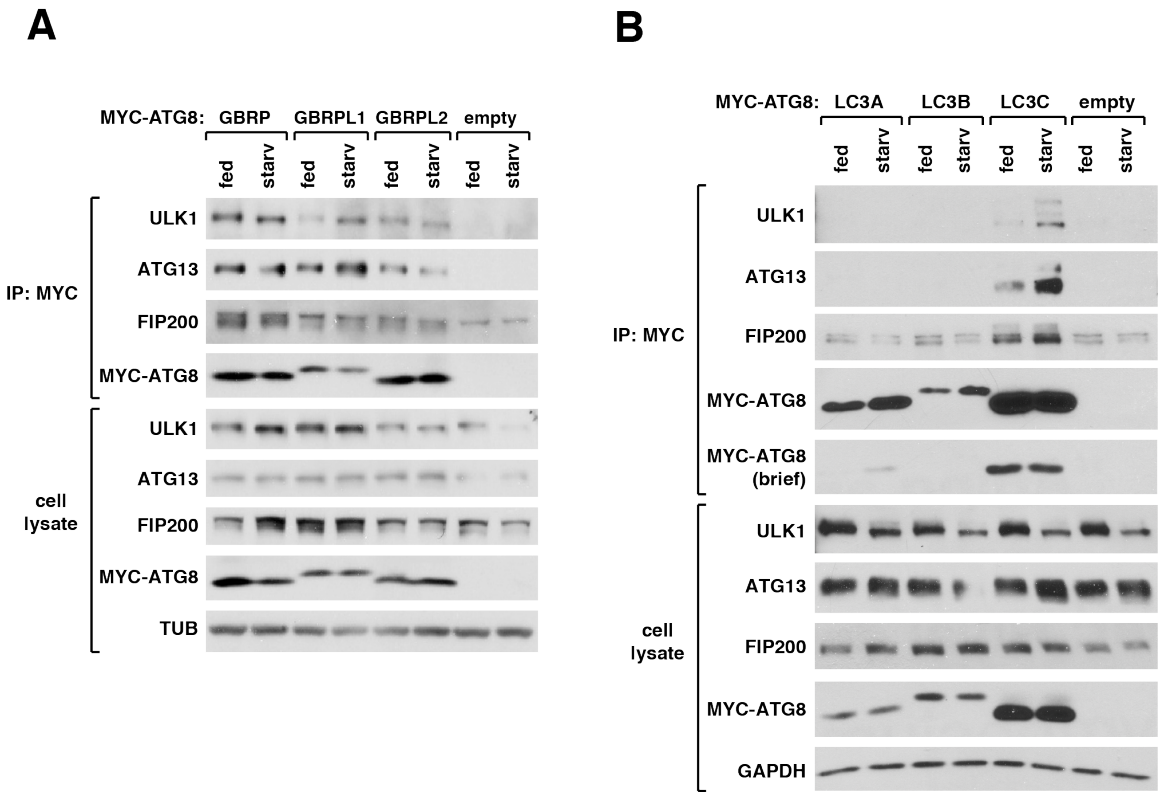

Figure 9. GABARAP proteins interact with the ULK1 complex independent of nutrient condition. (A) The binding affinity of GABARAP proteins for the ULK1 complex is not drastically changed by starvation. HEK293T cells transiently expressing the indicated MYC-tagged GABARAP proteins (or empty pRK5 as a negative control) were cultured in full medium (fed) or starved with EBSS (starv) for 2 h. MYC-tagged GABARAPs were immunoprecipitated using anti-MYC antibody. Co-immunoprecipitated endogenous ULK1, ATG13, and FIP200 were assessed by WB using the indicated antibodies. **(B)** The binding affinity of LC3C for the ULK1 complex is enhanced by starvation. Same procedure as described in (A), except the indicated MYC-tagged LC3 proteins were expressed.

2.4. ULK1 and ATG13 interact with one another independent of ATG8 binding

To understand the role of ATG8 binding to the ULK1 complex, we investigated the possibility that ATG8 binding to ULK1 or ATG13 might affect the interaction between ULK1 and ATG13, a constitutive interaction that is essential for ULK1 to associate with and phosphorylate target proteins and for autophagy [32–34,59]. To test whether ATG8 binding affects the ULK1-ATG13 interaction, ULK1 LIR mutant or ATG13 LIR mutant proteins were transiently expressed in HEK293T cells and the co-immunoprecipitation of co-expressed wild type ATG13 or ULK1 (respectively) was assessed.

HA-ULK1 was co-immunoprecipitated with MYC-ATG13 wild type (WT) and LIR mutant (MUT) at comparable levels (**Figure 10A**). Similarly, HA-ATG13 was co-immunoprecipitated with MYC-ULK1 wild type and LIR mutant at comparable levels, relative to the total MYC-ULK1 protein isolated (**Figure 10B**). Indeed, the binding of co-expressed HA-GABARAP was reduced for both LIR mutants (**Figure 10A and 10B**). Together, these results suggest that the binding of GABARAP to ULK1 or ATG13 is not required for the ULK1-ATG13 interaction.

For additional evidence that ATG8 binding to the ULK1 complex does not regulate the ULK1-ATG13 interaction, we tested whether co-expressing recombinant GABARAP along with recombinant ULK1 and ATG13 would affect the ULK1-ATG13 interaction. Transiently expressed MYC-ATG13 was immunoprecipitated from cells co-expressing HA-ULK1 alone or HA-ULK1 with HA-GABARAP. Indeed, HA-GABARAP was co-immunoprecipitated with MYC-ATG13 (**Figure 10C**). Importantly, the addition of HA-GABARAP had no effect on amount of co-immunoprecipitated HA-ULK1 (**Figure 10C**), indicating that GABARAP binding does not regulate the ULK1-ATG13 interaction.

FIGURE 10

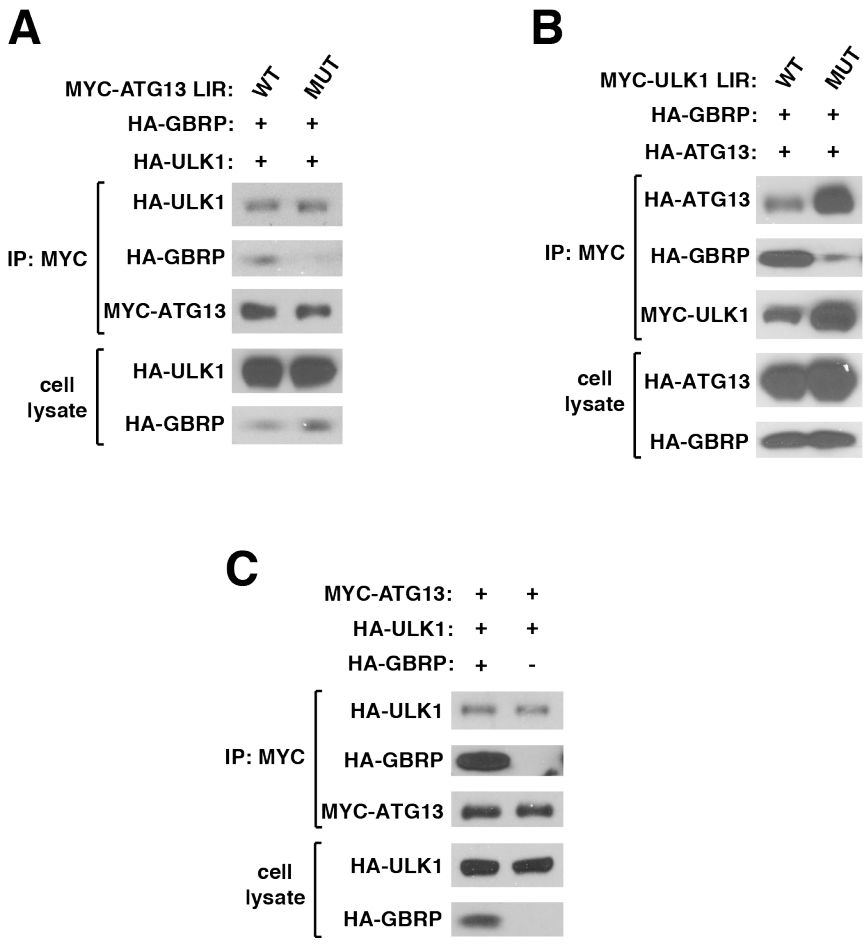

Figure 10. ULK1 and ATG13 interact with one another independent of GABARAP binding. (A) GABARAP binding to ATG13 is not required for the ULK1-ATG13 interaction. HA-ULK1 and HA-GABARAP were transiently co-expressed with MYC-ATG13 wild type (WT) or LIR mutant (MUT) in HEK293T cells. MYC-ATG13 variants were immunoprecipitated with anti-MYC antibody and co-immunoprecipitated HA-ULK1 and HA-GABARAP were assessed by WB. **(B)** GABARAP binding to ULK1 does not regulate the ULK1-ATG13 interaction. Same procedure as described in (A), except using HA-ATG13 and MYC-ULK1 variants. **(C)** GABARAP does not affect the ULK1-ATG13 interaction. MYC-ATG13 and HA-ULK1 were co-expressed with HA-GABARAP or empty pRK5. MYC-ATG13 was immunoprecipitated and co-immunoprecipitated HA-ULK1 and HA-GABARAP were assessed by WB.

2.5. Conclusion

In this chapter we clarified the interactions between members of the ULK1 complex and ATG8 proteins. We found that ATG8 proteins bind to the ULK1 complex with varying affinities. The ULK1 complex preferentially interacted with the GABARAP subfamily of proteins, although moderate interaction was detected with LC3C. Likewise, we found that members of the ULK1 complex vary in their affinity for ATG8 proteins. ATG13 interacted with the three GABARAP proteins and LC3C, while ULK1 only interacted with the GABARAP proteins. GABARAP binding to ATG13 did not require the ULK1 binding region of ATG13, suggesting that the binding is direct. Surprisingly, we did not observe interaction between any ATG8 and FIP200, indicating that ATG8 proteins interact with the ULK1 complex via binding to ATG13 and/or ULK1.

For insight into a possible role of the interaction, we examined the interaction in the autophagy-inducing condition of nutrient starvation. Starvation had a minimal effect on the binding of GABARAP proteins and the ULK1 complex. However, the binding of LC3C was drastically enhanced during starvation, indicating a potential role of the ULK1 complex-LC3C interaction in autophagy. Lastly, as a potential function of the interaction, we examined the possibility that ATG8 binding might affect the interaction between members of the ULK1 complex. We found that the ULK1-ATG13 interaction was unaffected by binding of either protein to GABARAP, suggesting that ATG8 binding to ULK1 or ATG13 does not play a role in the interaction between ULK1 and ATG13.

CHAPTER 3

THE LC3 AND GABARAP SUBFAMILIES OF ATG8 HAVE OPPOSING ROLES IN AUTOPHAGY INITIATION

The finding that ATG8 proteins have differential binding affinities for the ULK1 complex raises the question of whether specific ATG8 proteins have distinct functions in regulating the ULK1 complex and autophagy initiation. To address this question, we analyzed how depletion of ATG8 proteins from human cells affects ULK1 function. ULK1 function was assayed by monitoring the phosphorylation of ATG14 at Ser29, the residue recently identified and defined by our lab as a direct target of ULK1 phosphorylation [59]. Importantly, this specific phosphorylation is important for VPS34 activity and isolation membrane biogenesis [59]. In brief, we found that LC3B and LC3C suppress whereas GABARAP and GABARAPL1 promote ULK1 activity and the formation of isolation membranes in human cells.

3.1. ATG8 proteins regulate ULK1 activity

Since GABARAP proteins bind to the ULK1 complex with relatively high affinity, we suspected that GABARAP proteins are important for regulating ULK1 function. To test this prediction, we used Transcription Activator-Like Effector Nucleases (TALEN) to deplete individual GABARAP proteins from HCT116 cells, a human colon cancer cell line that can be efficiently modified by gene editing that relies on homologous recombination [110–112]. The three GABARAP-depleted cell lines, and their wild type (WT) counterparts, were incubated in full medium or EBSS for 1 h to activate ULK1. The phosphorylation status of ATG14 at Ser29 (p-ATG14) was analyzed by western blotting using an antibody specific to the phosphorylation [59]. Cells depleted of GABARAP showed no drastic defect in p-ATG14 when compared to wild type cells (**Figure 11**). Similar results were observed with cells depleted of GABARAPL1 or GABARAPL2.

FIGURE 11

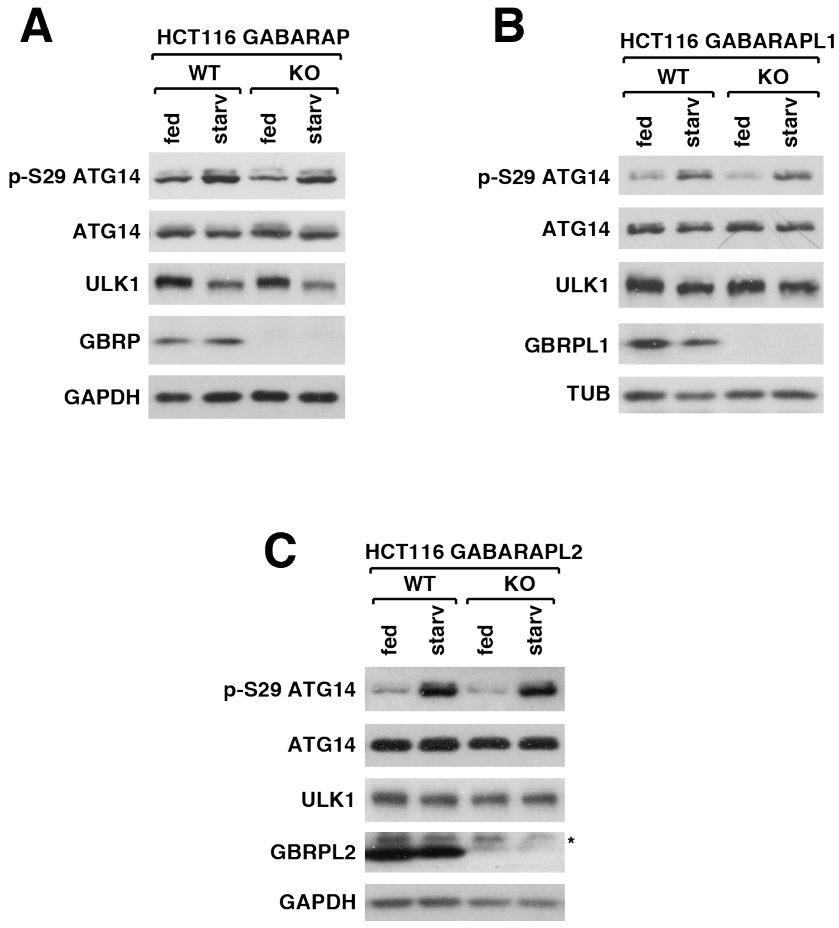

Figure 11. Individual GABARAP proteins are dispensable for ULK1 activity. (A) GABARAP is dispensable for ULK1 activity. Wild type (WT) or GABARAP-depleted (KO) HCT116 cells were cultured in full medium (fed) or starved with EBSS (starv) for 60 min. Cell lysates were collected and analyzed for ULK1 activity by WB using an antibody specific for phosphorylated ATG14 at Ser29. **(B)** GABARAPL1 is dispensable for ULK1 activity. Same procedure as described in (A), except GABARAPL1-depleted cells were used. **(C)** GABARAPL2 is dispensable for ULK1 activity. Same procedure as described in (A), except GABARAPL2-depleted cells were used. *Non-specific band for anti-GABARAPL2 (GBRPL2).

These results suggest that individually, GABARAP proteins are not essential for ULK1 activity. This implies that GABARAP proteins are either dispensable for ULK1 activation, or that GABARAP proteins might be functionally redundant in regulating ULK1 activity.

During this investigation another group reported using HeLa cells depleted of the three LC3 proteins, the three GABARAP proteins, or all six ATG8 proteins, referred to hereafter as LC3 TKO, GABARAP TKO, and Hexa KO cells, respectively [94]. We acquired these cells and tested them for ULK1 activation during nutrient starvation. Hexa KO cells showed an almost complete loss of p-ATG14 (**Figure 12A**). LC3 TKO cells showed a robust increase in p-ATG14 in both fed and starved conditions (**Figure 12A**). The increase of ATG14 phosphorylation in response to starvation was moderately blunted in the LC3 TKO cells, when compared to the WT. In contrast, GABARAP TKO cells showed a drastic reduction of p-ATG14, similar to that of the Hexa KO cells (**Figure 12A**), indicating that the effect of the Hexa KO is largely mediated by GABARAP proteins. These results suggest that GABARAP proteins are important for the phosphorylation of ATG14 at Ser29.

To further test whether ATG8 proteins regulate the activity of ULK1, we examined the phosphorylation of BECLIN 1 (BECN1) at Ser30, another modification recently identified and defined by our lab as a ULK1 phosphorylation that mediates VPS34 activity and isolation membrane biogenesis [58]. As with ATG14 phosphorylation, the phosphorylation of BECN1 at Ser30 was enhanced in the LC3 TKO cells and almost completely lost in the GABARAP TKO and Hexa KO cells, suggesting that ATG8 proteins regulate multiple phosphorylations of ULK1 (**Figure 12A**).

FIGURE 12

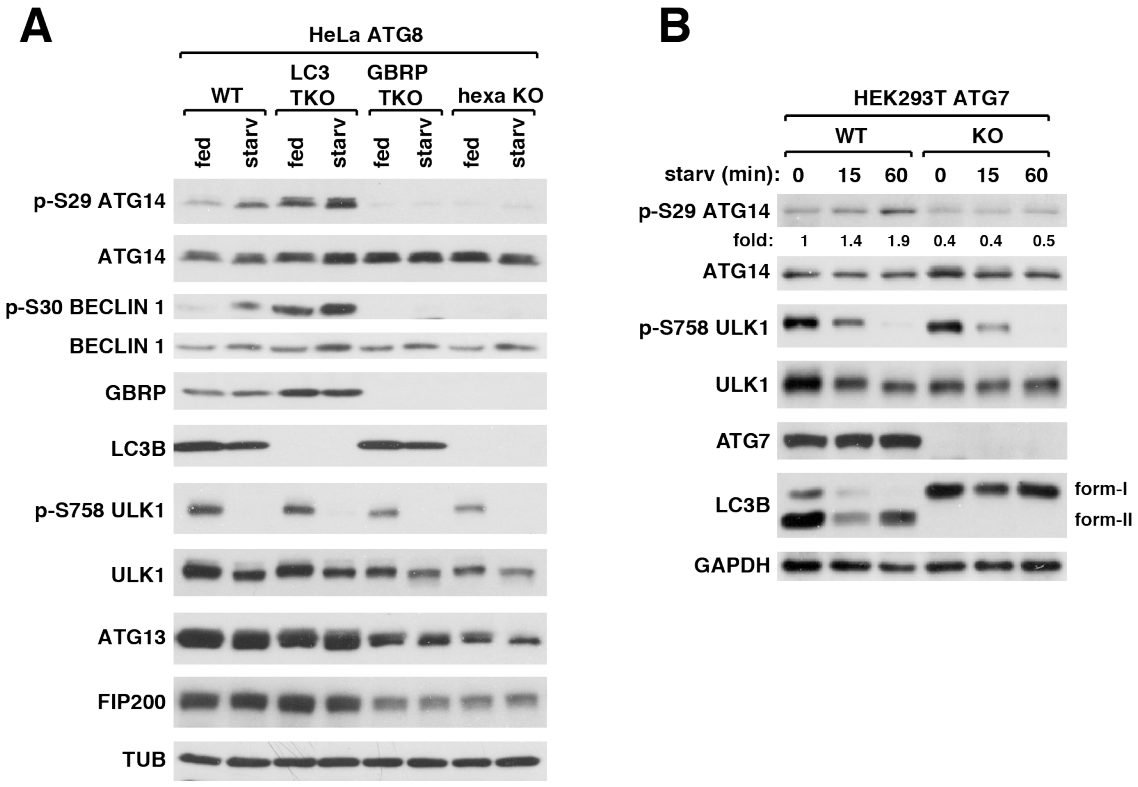

Figure 12. The GABARAP and LC3 subfamilies of ATG8 have opposing effects on ULK1 activity. (A) GABARAPs promote and LC3s suppress ULK1 activity. Wild type (WT), GABARAP TKO, LC3 TKO, or Hexa KO HeLa cells were cultured in full medium (fed) or EBSS (starv) for 60 min. As a measure of ULK1 activity, phosphorylated ATG14 and BECLIN1 were assessed using indicated antibodies. **(B)** PE conjugation of ATG8 positively regulates ULK1 activity. Wild type (WT) or ATG7-depleted (KO) HEK293T cells were cultured in full medium (0) or EBSS for 15 or 60 min and assessed for p-ATG14 by WB. Note: LC3B-II is PE conjugated and LC3B-I is not lipid conjugated.

As one possible mechanism for the differential effects of ATG8s on ULK1 activity, we considered the possibility that ATG8s might differentially regulate the phosphorylation of ULK1 at Ser758, a phosphorylation by mTORC1 that suppresses ULK1 activity [43]. However, when accounting for the levels of total ULK1 expression, the phosphorylation of ULK1 at Ser758 was not drastically different in cells depleted of ATG8s, suggesting that ATG8 proteins do not regulate ULK1 activity by regulating the phosphorylation of ULK1 by mTORC1 (**Figure 12A**).

Together, these results suggest that the GABARAP and LC3 subfamilies have distinct roles in regulating ULK1 signaling. GABARAP proteins appear to be important for the activity of ULK1, whereas LC3 proteins are not necessary for the activity of ULK1, but rather, might act as negative regulators.

Next, we asked if phosphatidylethanolamine (PE) conjugation of ATG8s contributes to their regulation of ULK1 activity. The HEK293T cells depleted of ATG7 (from Figure 8) were utilized to address this question. Relative to wild type cells, ATG7-depleted (KO) cells exhibited reduced p-ATG14 in both the fed and starved condition (**Figure 12B**). This result suggests that the PE conjugation of ATG8 is important for ULK1 activity. Unlike ATG8 Hexa KO cells that showed almost no p-ATG14 (**Figure 12A**), ATG7 KO cells showed only diminished p-ATG14. This indicates that the function of ATG8 proteins in regulating ULK1 activity is at least partially independent of their PE conjugation status.

3.2. GABARAP and GABARAPL1 promote ULK1 activity

In order to determine which ATG8 proteins are responsible for such differential effects on the activity of ULK1, we stably reintroduced individual ATG8s in the TKO cell lines using a lentiviral system and analyzed the phosphorylation of p-ATG14. Stable re-

expression of either GABARAP or GABARAPL1, but not GABARAPL2, in the GABARAP TKO cells was sufficient to restore p-ATG14 (**Figure 13**), suggesting that GABARAP and GABARAPL1 share a redundant function in promoting ULK1 activity. This result is consistent with our previous finding that depletion of GABARAP or GABARAPL1 alone did not affect ULK1 activity (**Figure 11A and 11B**), demonstrating the compensatory nature of GABARAP and GABARAPL1.

In addition to suppressed ULK1 activity, the GABARAP TKO cells showed a reduction of ULK1 expression, which might explain how ULK1 activity is reduced (**Figure 12A**). Supporting this notion, we found that reconstitution of GABARAP or GABARAPL1 in GABARAP TKO cells restored ULK1 expression to a level comparable to that of WT (**Figure 13**). However, reconstitution of GABARAPL2, which was also sufficient to restore ULK1 expression, failed to restore p-ATG14. This result suggests that restoration of ULK1 expression in GABARAP TKO cells is not sufficient to restore p-ATG14, and thus, GABARAP and GABARAPL1 might mediate ULK1 activity not simply through promoting ULK1 expression.

3.3. LC3B and LC3C negatively regulate GABARAP expression and ULK1 activity

We also analyzed the effects of reconstitution of LC3 members into LC3 TKO cells. Re-expression of either LC3B or LC3C in the LC3 TKO cells drastically reduced p-ATG14 (**Figure 14A**). Interestingly, re-expression of LC3A, which has a greater binding affinity for the ULK1 complex than LC3B, had a less apparent effect on p-ATG14. These results indicate that LC3B and LC3C, but not LC3A, might function to negatively regulate the ULK1 activity.

FIGURE 13

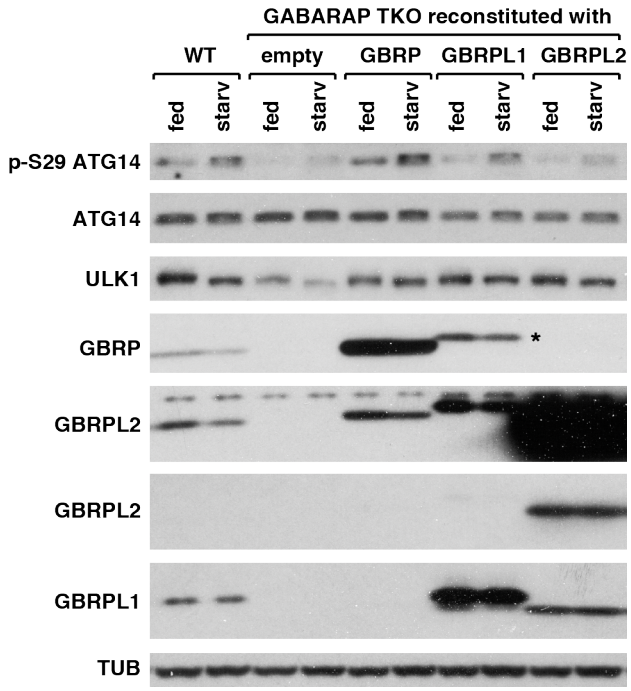

Figure 13. GABARAP and GABARAPL1 promote ULK1 activity. Individual GABARAPs were stably reconstituted in GABARAP TKO HeLa cells. Cells were cultured in full medium or EBSS for 60 min and cell lysates were assessed for p-ATG14 by WB. *GABARAPL1 cross-reacted with anti-GABARAP antibody

FIGURE 14

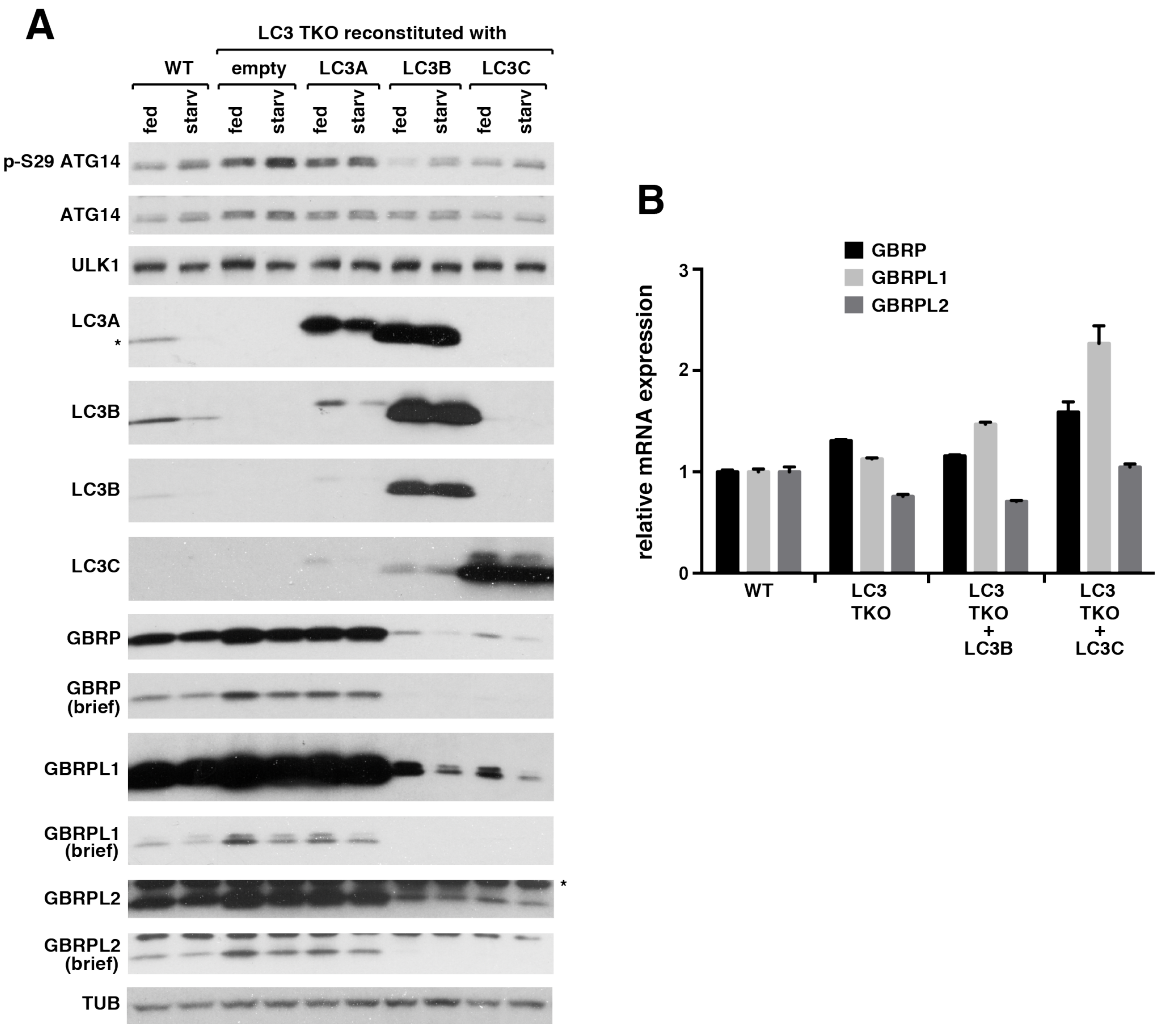

Figure 14. LC3B and LC3C suppress ULK1 activity and the expression of GABARAP proteins. (A) Individual LC3s were stably reconstituted in LC3 TKO HeLa cells. Cells were cultured in full medium or EBSS for 60 min and cell lysates were assessed for p-ATG14 by WB. *LC3B cross-reacted with anti-LC3A antibody and non-specific band for anti-GABARAPL2. **(B)** The effect of LC3B and LC3C on the protein expression of GABARAPs does not correlate with mRNA expression of GABARAPs. mRNA levels were quantified by qRT-PCR and normalized to GAPDH. n=3. RNA extracts were collected from the indicated LC3 TKO cell lines in the fed condition.

We noticed that GABARAP protein expression was increased in the LC3 TKO cells, suggesting that LC3 proteins downregulate GABARAP protein expression (**Figure 12A**). Interestingly, the re-expression LC3B or LC3C, but not LC3A, reduced GABARAP protein expression, which directly correlates with their effect on p-ATG14 (**Figure 14A**). Thus, it is possible that LC3B and LC3C suppress ULK1 activity by down-regulating the ULK1 activator GABARAP. To understand how LC3B and LC3C downregulate GABARAP protein expression, the mRNA levels of the three GABARAPs in the LC3B and LC3C reconstituted cells were assessed by qRT-PCR (quantitative reverse transcription – polymerase chain reaction). The effect of LC3B and LC3C re-expression on GABARAP protein expression did not correlate with an similar effect on GABARAP mRNA expression (**Figure 14B**). This indicates that the mechanism by which LC3B and LC3C regulate GABARAP protein expression is not via transcription of GABARAPs.

3.4. GABARAPs are required for starvation-induced isolation membrane biogenesis and autophagy activity

Given our results that GABARAPs and LC3s differentially regulate the activity of ULK1, we tested whether the differential effects are corroborated by changes in the formation of isolation membranes, the early membrane structures that develop into autophagosomes. To quantify isolation membranes, we performed immunostaining using an antibody against WIPI2. WIPI2 is enriched at isolation membranes and is commonly stained for to detect isolation membranes [74]. As expected, nutrient starvation drastically increased the number of WIPI2-positive puncta in wild type cells (**Figure 15**). The number of WIPI2-positive puncta was also significantly increased in response to starvation in LC3 TKO cells, suggesting that LC3 proteins are not essential for starvation-induced isolation membrane biogenesis (**Figure 15B**).

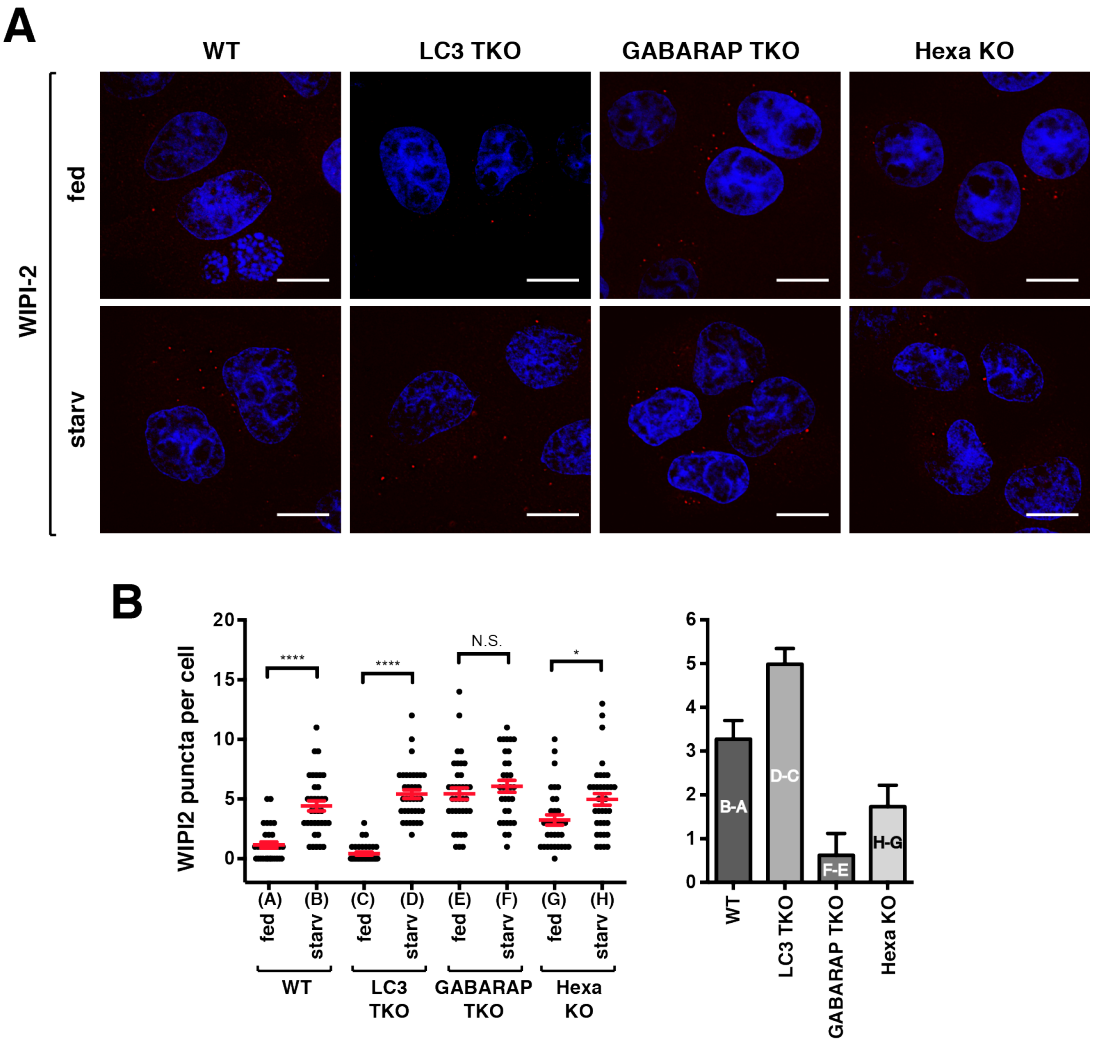

Figure 15. GABARAPs are important for isolation membrane biogenesis during starvation. (A) WT, LC3 TKO, GABARAP TKO, or Hexa KO HeLa cells were cultured in full medium or EBSS for 60 min. Endogenous WIPI-2 (red) was detected by immunostaining using anti-WIPI2 antibody (Millipore, MABC91). Nuclei were stained with DAPI (blue). Scale bar: 10μm. **(B)** Quantitative analysis of (A). Red bars are mean +/- SEM (*$p < 0.05$; ****$p < 0.0001$; N.S. is not significant; 2-way ANOVA with Sidak's post-hoc, n>30).

This result suggests that LC3s are not required for isolation membrane biogenesis, but rather, might suppress isolation membrane biogenesis in response to starvation. This effect might be related to the higher activity of ULK1 in LC3 TKO cells.

In contrast, GABARAP TKO cells showed an elevated number of WIPI2-positive puncta in the fed condition relative to wild type cells. However, number of puncta was not significantly increased with by starvation (**Figure 15A and 15B**). This result suggests that GABARAPs are important for cells to induce isolation membrane biogenesis in response to starvation and might suppress isolation membrane biogenesis in the fed condition.

We also tested how ATG8 proteins affect autophagy activity. SQSTM1 (also known as p62) and PE-conjugated ATG8s (form-II) are substrates of autophagy and their degradation (flux) is commonly used as an assay for autophagy activity. By monitoring SQSTM1 and ATG8 levels in the presence or absence of the autophagy inhibitor bafilomycin A1 (BAFA1), we assessed autophagy activity. Depletion of all the three LC3 proteins from HeLa cells did not suppress the autophagic flux of GABARAPL1 (**Figure 16**). Compared to wild type cells, LC3 TKO cells showed a higher ratio of form-II to form-I of GABARAPL1, indicating that LC3s suppress the PE-conjugation of GABARAPL1. The autophagic flux of SQSTM1 in the LC3 TKO cells was comparable to that of wild type cells. In contrast, GABARAP TKO cells showed a reduction of LC3B-II flux. Furthermore, starvation failed to induce a decrease of SQSTM1 in the GABARAP TKO (**Figure 16**). This suggests that GABARAP proteins, but not LC3 proteins, are important for autophagy activity.

FIGURE 16

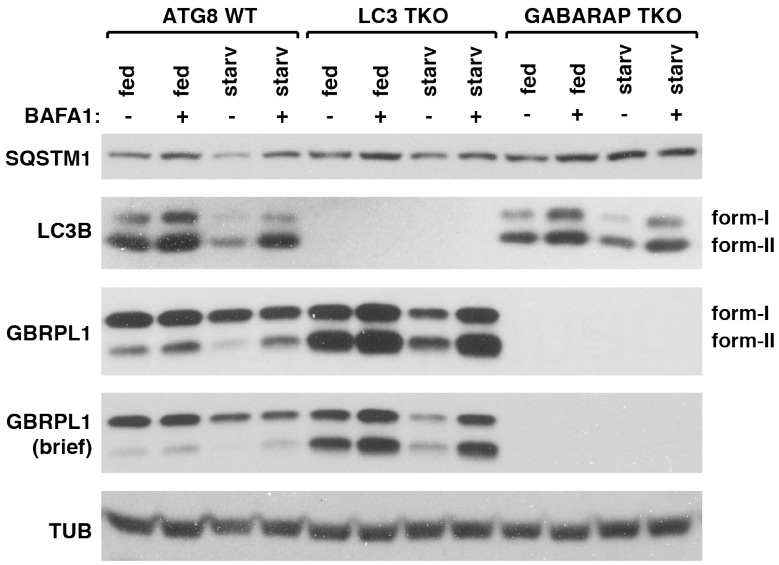

Figure 16. LC3 proteins are dispensable for the degradation of GABARAPL1 by autophagy. WT, LC3 TKO, or GABARAP TKO HeLa cells were cultured in full medium or EBSS for 2 h in the presence or absence of 100nM bafilomycin A1 (BAFA1). Cell lysates were collected and analyzed by WB using indicated antibodies. Note: form-II is conjugated with PE, form-I is not.

3.5. Conclusion

In this chapter we investigated the function of ATG8 proteins in ULK1 activation and autophagy. Using HeLa cells depleted of various ATG8 proteins, we found that the LC3 subfamily negatively regulates ULK1 activity, whereas the GABARAP subfamily positively regulates ULK1 activity and autophagy initiation. Furthermore, through reconstitution experiments we identified LC3B and LC3C as the LC3 proteins responsible for suppressing ULK1, and GABARAP and GABARAPL1 as the GABARAP proteins responsible for promoting ULK1 activity. Combined with our individually depleted GABARAP cell results, we found that GABARAP and GABARAPL1 function redundantly in promoting ULK1 activity. This is the first study to demonstrate opposing roles between LC3 and GABARAP subfamilies in regulating ULK1 activity and autophagy initiation and marks and important step in understanding how the ULK1 complex and autophagy initiation is regulated.

CHAPTER 4

ATG8 BINDING TO ULK1 AND ATG13 IS IMPORTANT FOR AUTOPHAGY INITIATION

Given that GABARAP proteins bind to and regulate the ULK1 complex, we wondered about the functional significance of the GABARAP-ULK1 complex interaction. As both ULK1 and GABARAP function in autophagy, we hypothesized that their interaction plays a role in autophagy. We suspected that the function of GABARAPs in promoting ULK1 activity requires their physical interaction with ULK1. To test this hypothesis, we disabled the interaction between ATG8 proteins and ULK1 complex members by mutating their LIRs. We found that ATG8 binding to ULK1 positively regulates ULK1 function and the biogenesis of isolation membranes and autophagosomes in response to starvation. We also found that ATG8 binding to ATG13 positively regulates ULK1 activity, whereas ATG8 binding to FIP200 does not play a role in ULK1 activation or autophagy.

4.1. ATG8 binding to ULK1 is important for autophagy activity

To address the role of the ATG8 binding to ULK1, we disrupted the ULK1-ATG8 interaction by introducing point mutations in the LIR of endogenous ULK1 in HCT116 cells using CRISPR-Cas9-assisted genome editing. The successful mutations were verified by DNA sequencing (**Figure 17A**). In the fed state, the ULK1 LIR mutant cells showed elevated levels of SQSTM1, implying defective basal autophagy. Unlike in WT cells, the level of SQSTM1 in the fed state of the mutant cells was not significantly increased by BAFA1, suggesting that basal autophagy is defective (**Figure 18A and 18C**). Furthermore, the autophagy-dependent degradation of SQSTM1 and LC3-II in response to starvation was significantly reduced in ULK1 LIR mutant cells (**Figure 18A-18C**).

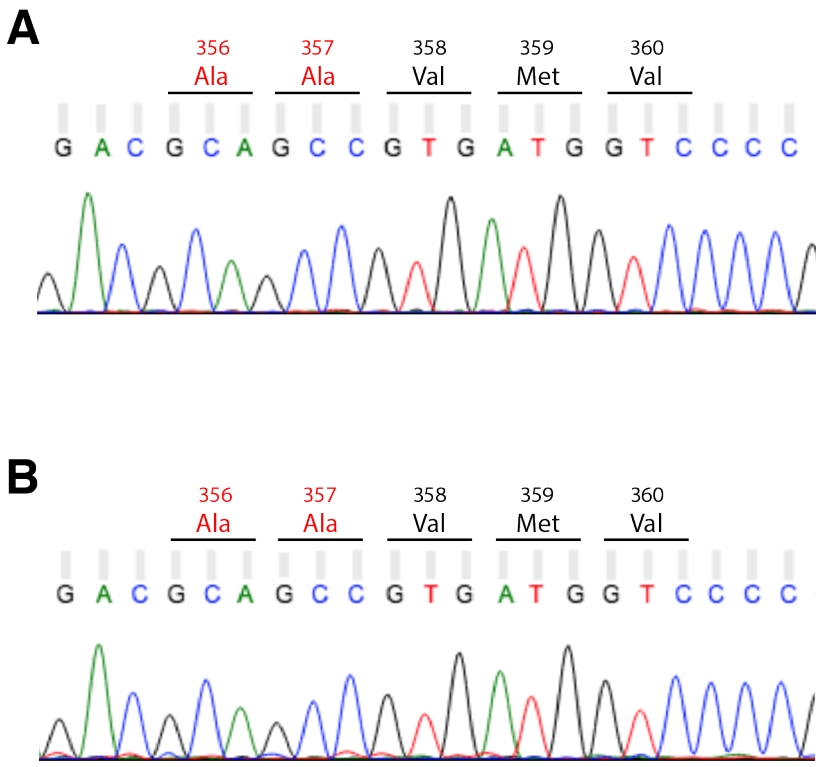

Figure 17. Confirmation of ULK1 LIR genomic mutation. Sequencing of the ULK1 LIR for HCT116 cells **(A)** and HEK293T cells **(B)** confirms codons were replaced with those encoding Alanine (shown in red). Sequencing chromatograms shown were modified from those obtained from the sequencing provider, GENEWIZ, Inc.

FIGURE 18

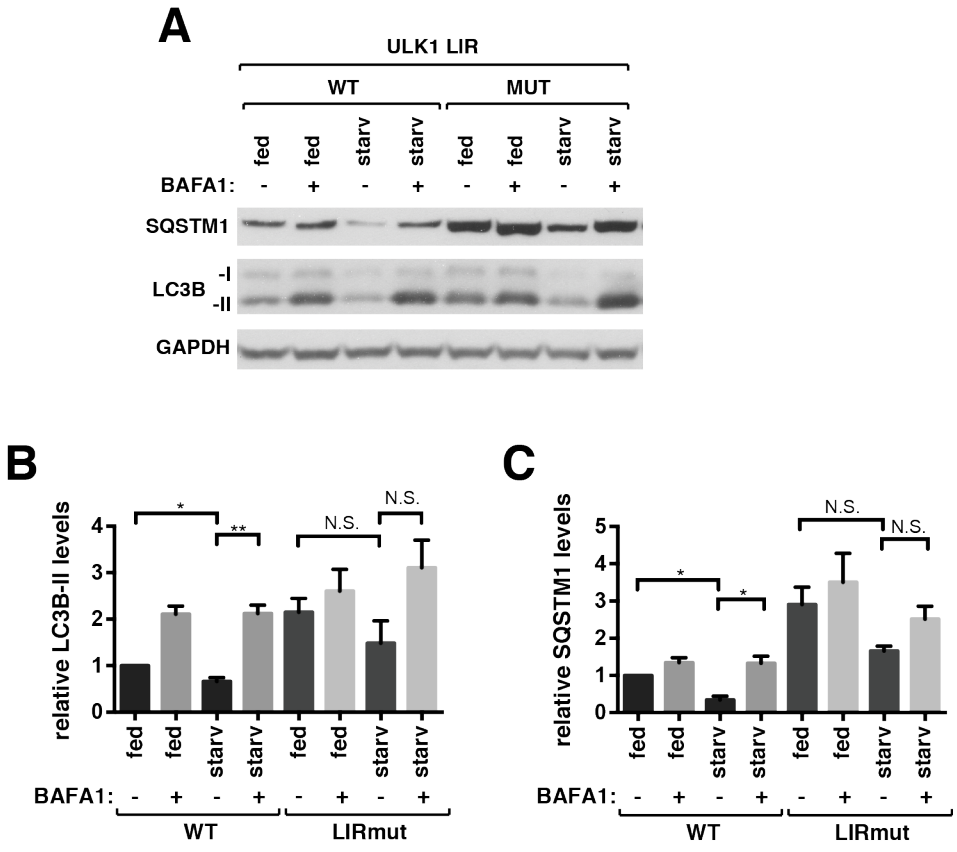

Figure 18. ATG8 binding to ULK1 is important for autophagy flux. (A) Wild type (WT) or ULK1 LIR mutant (MUT) HCT116 cells were cultured in full medium (fed) or EBSS (starv) for 2 h in the presence or absence of 100nM bafilomycin A1 (BAFA1). Whole-cell extracts were collected and analyzed by WB using indicated antibodies. **(B-C)** Quantitative analysis of LC3B-II and SQSTM1 from (A). Error bars are +/- SEM (*$p < 0.05$; **$p < 0.01$; Student t-test, n=3 independent experiments).

These results suggest that ATG8 binding to ULK1 is necessary for basal and starvation-induced autophagy activity.

4.2. ATG8 binding to ULK1 is important for isolation membrane and autophagosome biogenesis during starvation

To determine how the autophagic flux of autophagy substrates is compromised in the ULK1 LIR mutant cells, we examined the number of autophagosomes by immunostaining endogenous LC3B. Compared with wild type cells, the steady state number of LC3B-positive puncta was higher in ULK1 LIR mutant cells (**Figure 19A and 19B**). However, unlike with wild type cells where starvation significantly increased the number of LC3B puncta, the mutant cells did not show a significant increase in the number of LC3B puncta, indicating that starvation-induced autophagosome biogenesis is compromised or that autophagosome turnover is enhanced in the mutant cells. Blocking autophagosome-lysosome fusion with BAFA1 prevents the degradation of autophagosomes, thereby causing them to accumulate [113]. Thus, BAFA1 allows for the assessment of autophagosome biogenesis and turnover. Without BAFA1, the number of LC3B puncta was not significantly different between WT and ULK1 LIR mutant cells. However, in the presence of BAFA1, there were significantly fewer LC3B puncta in the mutant, suggesting that fewer autophagosomes accumulated in the mutant (**Figure 19A and 19B**). Together, these results suggest that ATG8 binding to ULK1 is important for starvation-dependent autophagosome biogenesis and turnover. To understand how ATG8 binding to ULK1 promotes autophagosome biogenesis, we assessed isolation membrane biogenesis by immunostaining WIPI2 during starvation. The ULK1 LIR mutation showed a more striking effect on WIPI2 puncta than on LC3B puncta, significantly and drastically suppressing the formation of WIPI2 puncta upon starvation (**Figure 20A and 20B**). These results suggest that ATG8 binding to ULK1 is important for starvation-induced isolation membrane biogenesis.

FIGURE 19

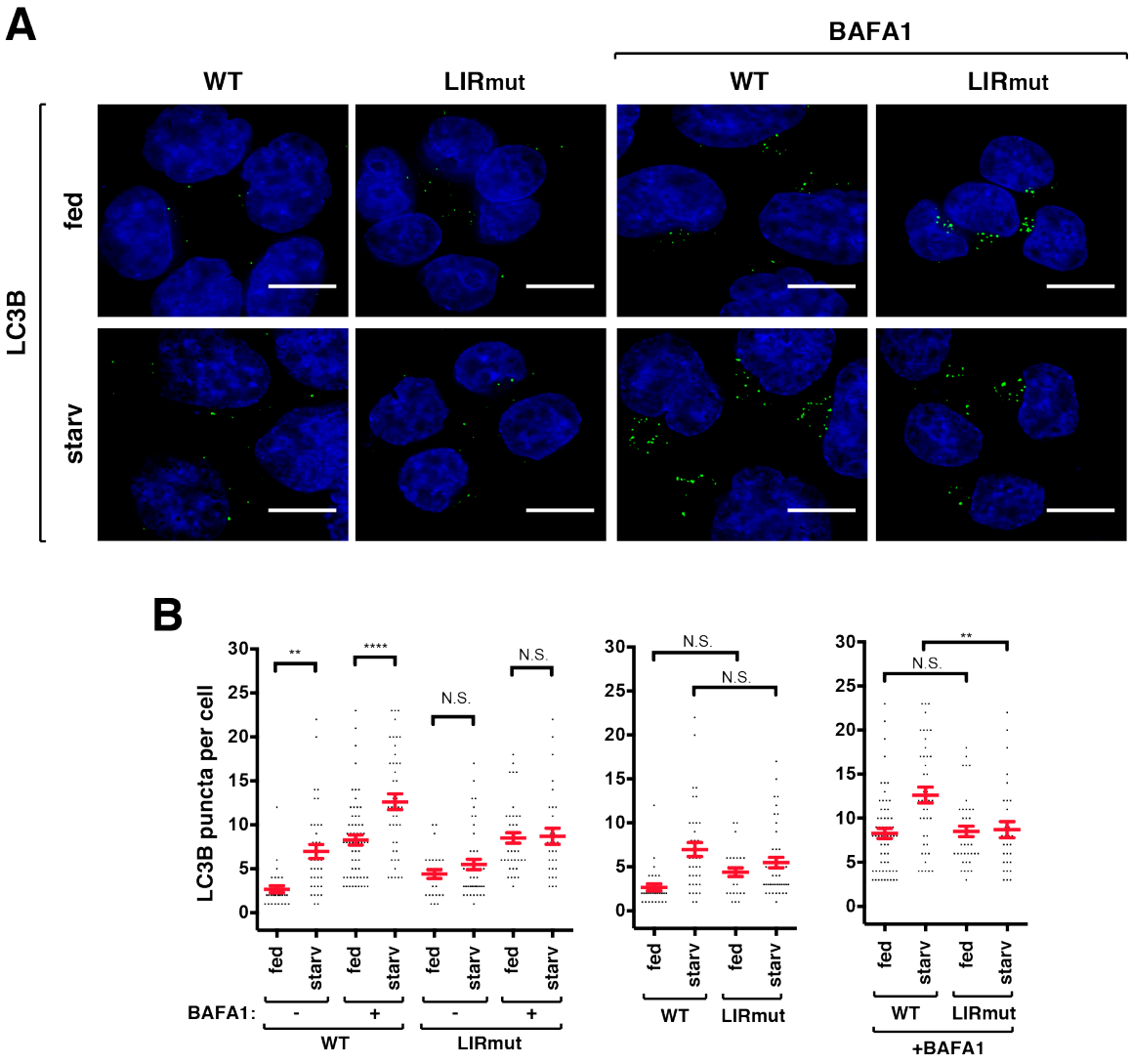

Figure 19. ATG8 binding to ULK1 is important for autophagosome biogenesis and turnover. (A) WT or ULK1 LIR mutant HCT116 cells were cultured in full medium or EBSS for 2 h in the presence or absence of 100nM bafilomycin A1. Endogenous LC3B (green) was detected by immunostaining using anti-LC3B antibody (MBL, PM036). Nuclei were stained with DAPI (blue). Scale bar: 10μm. **(B)** Quantitative analysis of (A). Red bars are mean +/- SEM (**$p < 0.01$; ****$p<0.0001$; 2-way ANOVA with Sidak's post-hoc, n=27).

FIGURE 20

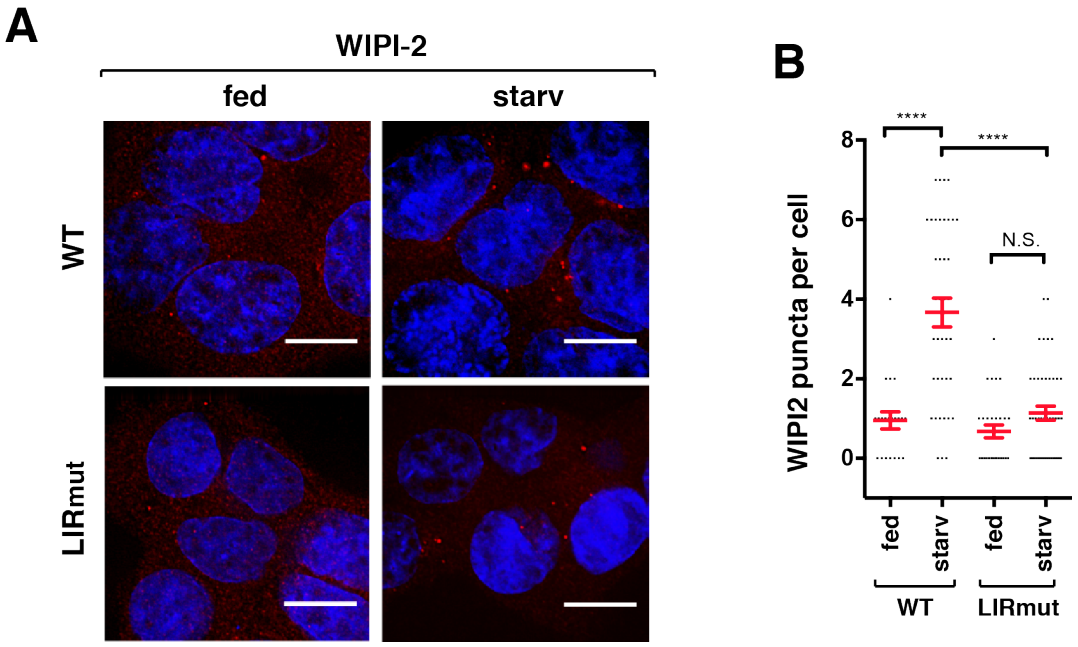

Figure 20. ATG8 binding to ULK1 is important for starvation-induced isolation membrane biogenesis. (A) WT or ULK1 LIR mutant HCT116 cells were cultured in full medium or EBSS for 60 min. Endogenous WIPI-2 (red) was detected by immunostaining using anti-WIPI-2 antibody (Millipore, MABC91). Nuclei were stained with DAPI (blue). Scale bar: 10μm. **(B)** Quantitative analysis of (A). Red bars are mean +/- SEM (****p<0.0001; Student t-test, n > 20).

4.3. ATG8 binding to ULK1 is important for ULK1 puncta during starvation

Upon starvation, ULK1 condenses at the ER to form puncta that mark sites of autophagosome nucleation [38,39]. To determine if ATG8 binding regulates ULK1 puncta formation, we immunostained endogenous ULK1 WT and LIR mutant. The antibody was confirmed to be specific to ULK1 prior to the experiment (**Figure 21A and 21B**). As expected, the number of wild type ULK1 puncta was significantly increased with starvation (**Figure 22A and 22B**). Importantly, relative to the wild type, there were significantly fewer ULK1 LIR mutant puncta during starvation (**Figure 22A and 22B**). This result indicates that ATG8 proteins, by binding to ULK1, facilitate ULK1 condensation during starvation.

4.4. ATG8 binding to ULK1 is important for ULK1 activity

Given that ATG8 binding to ULK1 is important for the formation of isolation membranes, a process that requires ULK1 activity, we predicted that ATG8 binding to ULK1 is important for ULK1 activity. In support of this prediction, the phosphorylation of ATG14 at Ser29 was drastically diminished in ULK1 LIR mutant cells relative to wild type cells (**Figure 23A**). Similar to the phosphorylation of ATG14, the starvation-dependent phosphorylation of ATG13 at Ser355 was reduced in ULK1 LIR mutant cells (**Figure 23B**), suggesting that ATG8 binding to ULK1 positively regulates the phosphorylation of multiple ULK1 substrates. To test if ATG8 binding to ULK1 is important for ULK1 activity in non-cancer human cells, the ULK1 LIR mutation was introduced in HEK293T cells using CRISPR-Cas9 (**Figure 17B**). As observed with HCT116 cells, disrupting the ULK1-ATG8 interaction in HEK293T cells reduced p-ATG14 (**Figure 23C**).

FIGURE 21

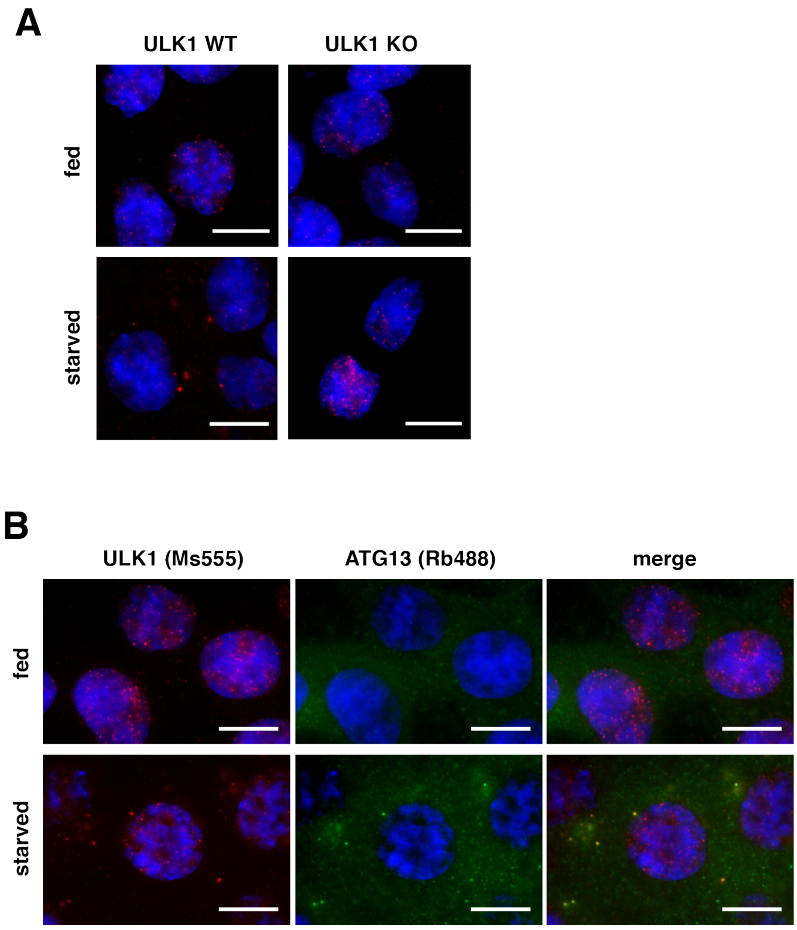

Figure 21. Validation of ULK1 antibody used for immunostaining. Identification of ULK1-specific puncta. **(A)** Wild type (WT) or ULK1-depleted (KO) HCT116 cells were cultured in full medium (fed) or EBSS (starved) for 60 min. Endogenous ULK1 (red) was detected by immunostaining using the anti-ULK1 antibody (Santa Cruz Biotechnology, sc-390904). The absence of ULK1 protein in the ULK1 KO cells was previously verified by WB [59]. Note: cytosolic puncta are specific to ULK1 whereas nuclear staining is non-specific. **(B)** Further validation that anti-ULK1 antibody is specific by co-staining ATG13. WT cells were treated as described in (A), except Atg13 (green) was also detected by co-immunostaining using anti-Atg13 antibody (Cell Signaling Technology, 13468). Nuclei are stained with DAPI (blue). Scale: 10μm. Images are non-deconvolved.

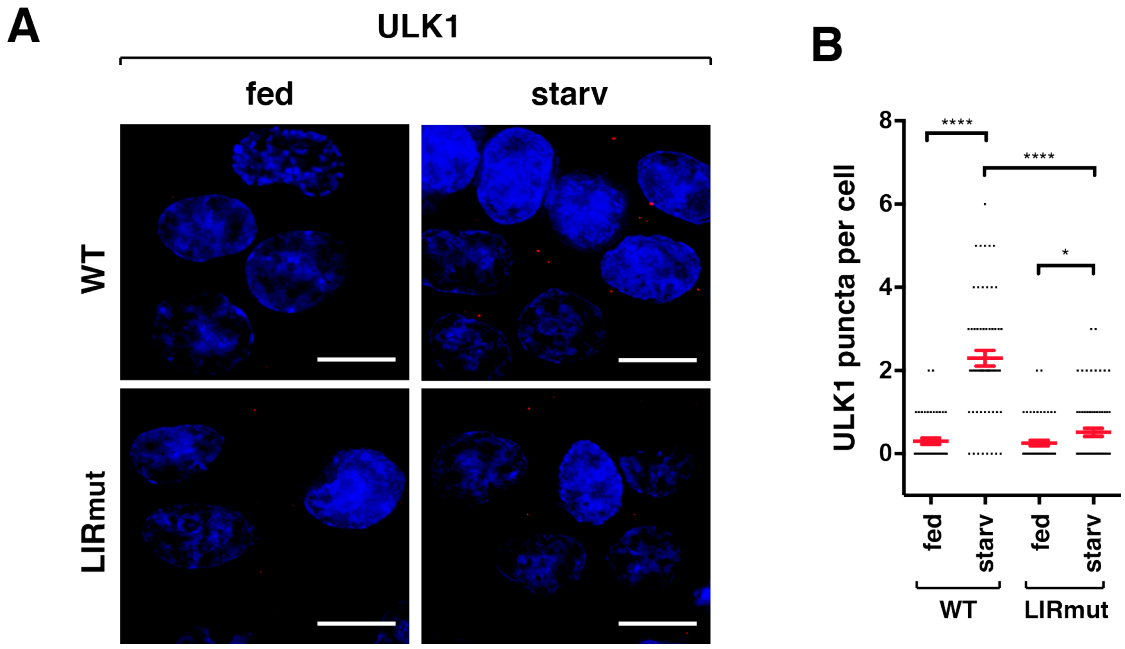

Figure 22. ATG8 binding to ULK1 is important for starvation-induced ULK1 puncta. (A) WT or ULK1 LIR mutant HCT116 cells were cultured in full medium or EBSS for 60 min. Endogenous ULK1 (red) was detected by immunostaining using anti-ULK1 antibody (Santa Cruz, sc-390904). Specificity of anti-ULK1 antibody was confirmed (Figure 21). Note: for image clarity, the red nuclear staining was removed from images shown above. Nuclei were stained with DAPI (blue). Scale bar: 10μm. **(B)** Quantitative analysis of (A). Red bars are mean +/- SEM (*$p < 0.05$; ****$p<0.0001$; Student t-test, $n \geq 50$).

FIGURE 23

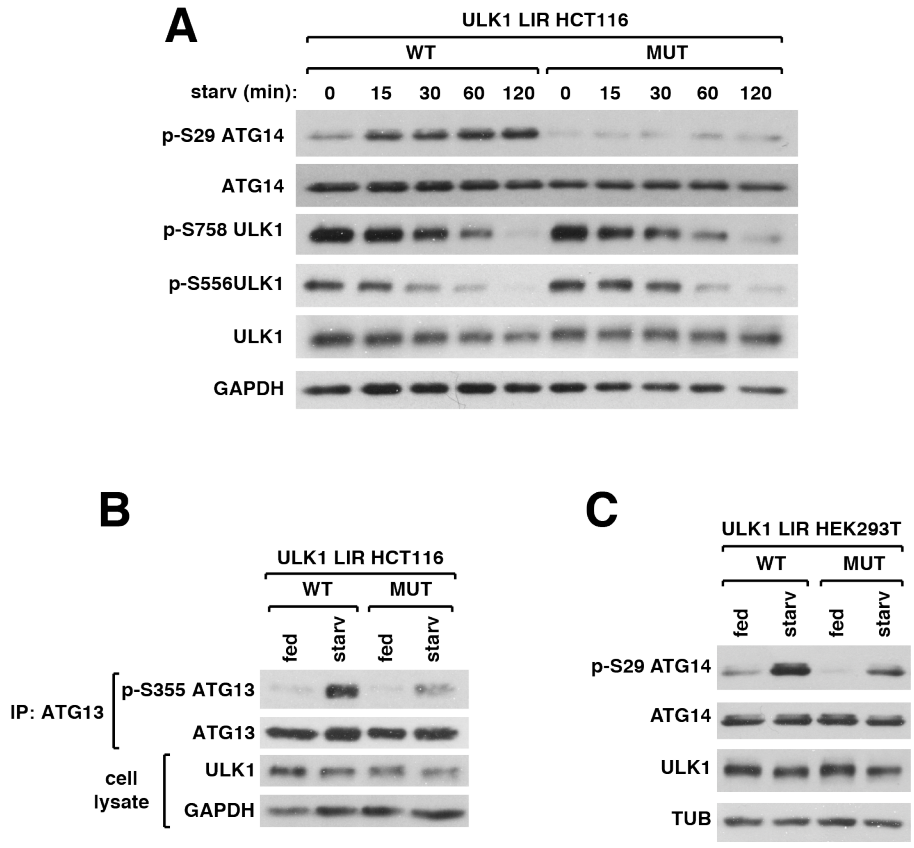

Figure 23. ATG8 binding to ULK1 is important for ULK1 activity. (A) ATG8 binding to ULK1 is important for the starvation-induced ULK1-mediated phosphorylation of ATG14. Wild type (WT) or ULK1 LIR mutant (MUT) HCT116 cells were cultured in full medium or EBSS for the indicated times. Cell lysates were collected and analyzed by WB using the indicated antibodies. **(B)** ATG8 binding to ULK1 is important for the starvation-induced ULK1-mediated phosphorylation of ATG13. WT or ULK1 LIR mutant HCT116 cells were cultured in full medium or EBSS for 60 min. ATG13 was enriched by immunoprecipitation using anti-ATG13 antibody (Cell Signaling Technology, 13468). Total and phosphorylated ATG13 at Ser355 were detected by WB. **(C)** ATG8 binding to ULK1 is important for ULK1 activation in HEK293T cells. WT or ULK1 LIR mutant HEK293T cells were cultured in full medium or EBSS for 60 min.

To understand how ATG8 binding to ULK1 promotes ULK1 activity, we tested if the LIR mutation affects the binding of ULK1 to ATG13, FIP200, or ATG101, interactions that are important for ULK1 activity [32–34]. The LIR mutation of ULK1 did not alter the interaction of ULK1 with ATG13, FIP200, or ATG101, indicating that the integrity of the ULK1 complex is intact in the mutant cells (**Figure 24A**). Next we tested whether the binding of ATG8 to ULK1 positively regulates the phosphorylation of ATG14 by promoting the association between ULK1 and ATG14. ULK1 associates with ATG14 via the ATG13-ATG14 interaction [59]. As the interaction between ATG13 and ATG14 is weak and transient [59], the chemical cross-linker DSP was used to stabilize the interaction. The LIR mutation of ULK1 did not alter the binding of ATG13 to ATG14 (**Figure 24B**), indicating that the ATG8 binding to ULK1 is unlikely to affect ULK1 substrate recognition. Interestingly, we observed that ULK1 LIR mutation reduced the interactions of GABARAP and GABARAPL1 with ATG13 and FIP200 (**Figure 25**), indicating that ATG8 binding ULK1 might facilitate ATG8 binding to ATG13 and FIP200, or at least that ATG8 binding to ULK1 contributes to the ATG8-ULK1 complex interaction. Although it is unclear how the binding of ATG8 to ULK1 regulates the activity of ULK1, the results above demonstrate for the first time that the ATG8 binding to ULK1 is important for ULK1 activation in response to starvation.

4.5. ATG8 binding to ATG13 is important for ULK1 activity

The observation that the binding of ATG8 to ATG13 and FIP200 was not completely abolished in the ULK1 LIR mutant cells suggests that ATG8 proteins can partially bind to the ULK1 complex through interacting with ATG13 and possibly FIP200 (**Figure 25**). To examine the role of ATG8 binding to ATG13, we attempted to introduce point mutations in the LIR of ATG13 in the HCT116 genome using CRISPR-Cas9 but were unsuccessful.

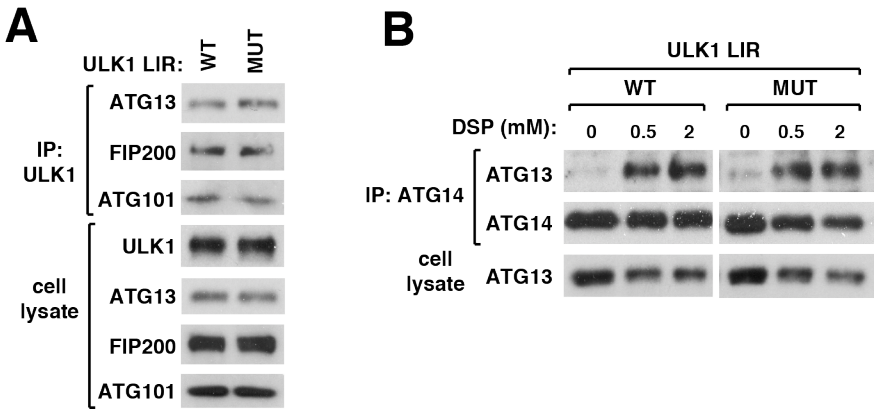

Figure 24. ATG8 binding to ULK1 is not required for ULK1 complex intra-association or association with ATG14. (A) ATG8 binding to ULK1 does not regulate the interaction between ULK1 complex members. ULK1 was isolated from wild type (WT) or ULK1 LIR mutant (MUT) HCT116 cells by immunoprecipitation using anti-ULK1 antibody (Santa Cruz, sc-10900). The levels of co-immunoprecipitated ULK1 complex members were analyzed by WB. **(B)** ATG8 binding to ULK1 does not regulate the interaction between ATG13 and ATG14. Wild type or ULK1 LIR mutant HCT116 cells were treated with dithiobis(succinimidyl propionate) (DSP) at the indicated concentrations for 10 min to crosslink protein interactions prior to collecting whole-cell extracts. ATG14 was immunoprecipitated using anti-ATG14 antibody (Santa Cruz, sc-164767) and co-immunoprecipitated ATG13 was assessed by WB.

FIGURE 25

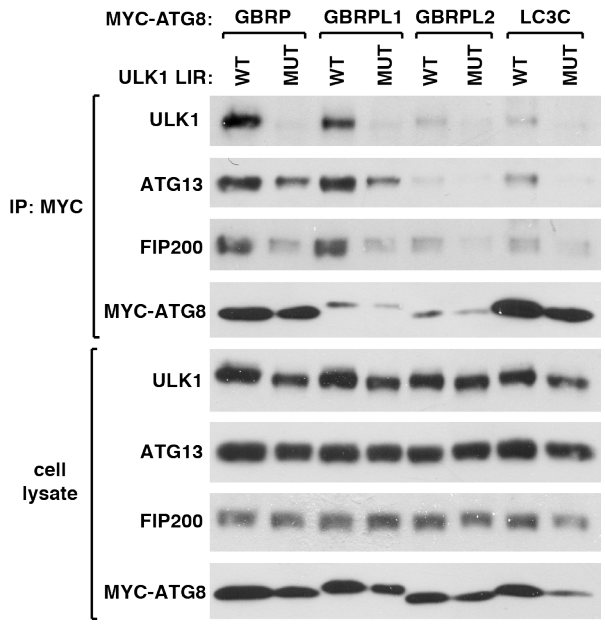

Figure 25. ATG8 binding to the ULK1 complex is reduced in ULK1 LIR mutant cells. The indicated MYC-ATG8 proteins were transiently expressed in wild type (WT) or ULK1 LIR mutant (MUT) HEK293T cells and immunoprecipitated with anti-MYC antibody. The amount of co-immunoprecipitated ULK1, ATG13, and FIP200 was assessed by WB.

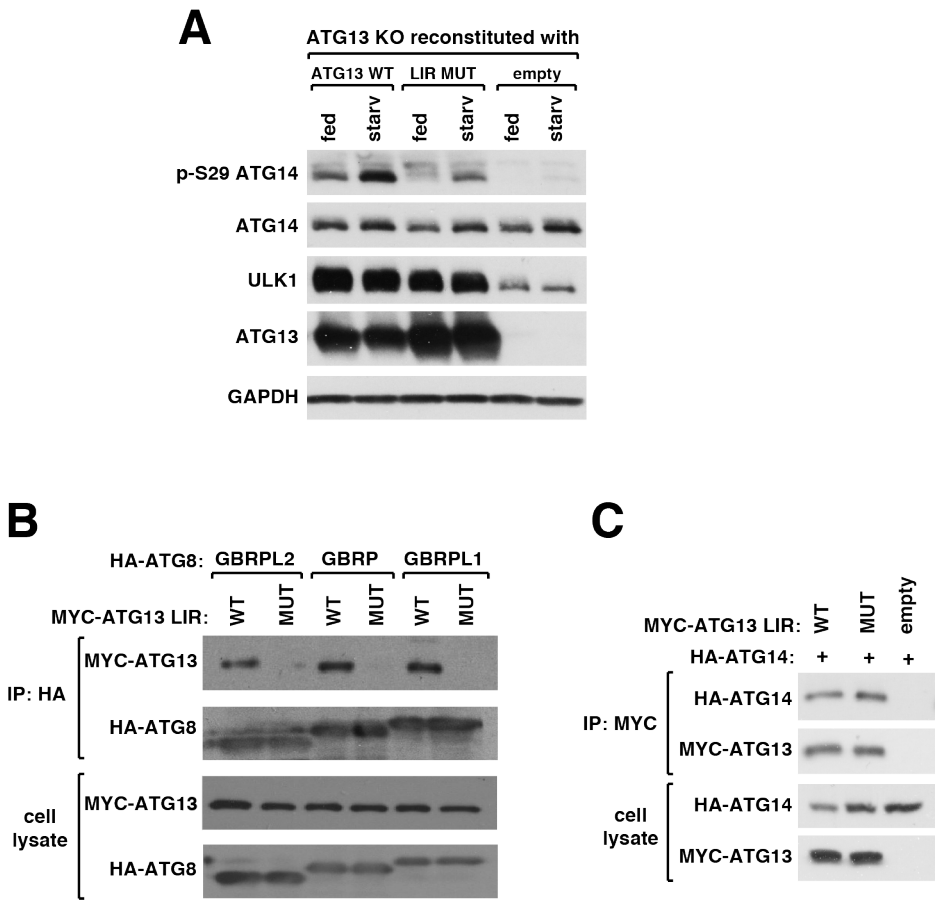

Figure 26. ATG8 binding to ATG13 is important for ULK1 activity. (A) Cells expressing ATG13 LIR mutant have reduced ULK1 activity. ATG13-depleted HCT116 cells stably expressing MYC-ATG13 wild type (WT), LIR mutant (MUT), or empty pRK5 were cultured in full medium (fed) or EBSS (starv) for 60 min. **(B)** Verification that ATG8 proteins do not bind the ATG13 LIR mutant. MYC-ATG13 wild type or LIR mutant were transiently co-expressed with HA-tagged GABARAP, GABARAPL1, or GABARAPL2 in HEK293T cells. HA-ATG8s were immunoprecipitated with anti-HA antibody and co-immunoprecipitated MYC-ATG13 was assessed by WB. **(C)** ATG8 binding to ATG13 is not required for the ATG13-ATG14 interaction. MYC-ATG13 wild type or LIR mutant were transiently co-expressed with HA-ATG14 in HEK293T cells. MYC-ATG13 was immunoprecipitated with anti-MYC antibody and co-immunoprecipitated HA-ATG14 was assessed by WB.

As an alternative approach, we stably reconstituted ATG13-depleted (KO) HCT116 cells with wild type ATG13 or the LIR mutant of ATG13, incapable of binding ATG8s (**Figure 26B**). Similar to ULK1 LIR mutant cells, cells expressing ATG13 LIR mutant showed reduced p-ATG14 (**Figure 26A**). This result indicates that ATG8 binding to ATG13 is important for the activation of ULK1. The mutational effect on the ULK1 activity was not due to any disruption of the interaction between ATG14 and ATG13 (**Figure 26C**).

We also generated HCT116 cells where point mutations were introduced in the LIR of endogenous FIP200 by the CRISPR-Cas9 technique (**Figure 27D**). In contrast to ULK1 and ATG13 LIR mutant cells, FIP200 LIR mutant cells showed no drastic change in p-ATG14 (**Figure 27A**). This result suggests that the binding of ATG8 to FIP200, even if it occurs, does not play a role in the activation of ULK1. Supporting the result, the FIP200 LIR mutation did not have any effect on autophagy flux (**Figure 27B**). Observing that p-ATG14 was not completely abolished in the ULK1 LIR mutant cells (**Figure 23A-23C**), we considered a possibility that ATG8 binding to FIP200 might partially compensate for the ATG8-ULK1 interaction in regards to ULK1 activity. To address this possibility, we mutated the LIR of ULK1 in the FIP200 LIR mutant cells using CRISPR-Cas9. The starvation-induced phosphorylation of ATG14 was suppressed in FIP200/ULK1 LIR mutant cells to a level similar to that of ULK1 LIR mutant cells (**Figure 27C**). Therefore, it does not appear that ATG8 binding to FIP200 compensates for loss of ATG8 binding to ULK1 in regards to ULK1 signaling.

FIGURE 27

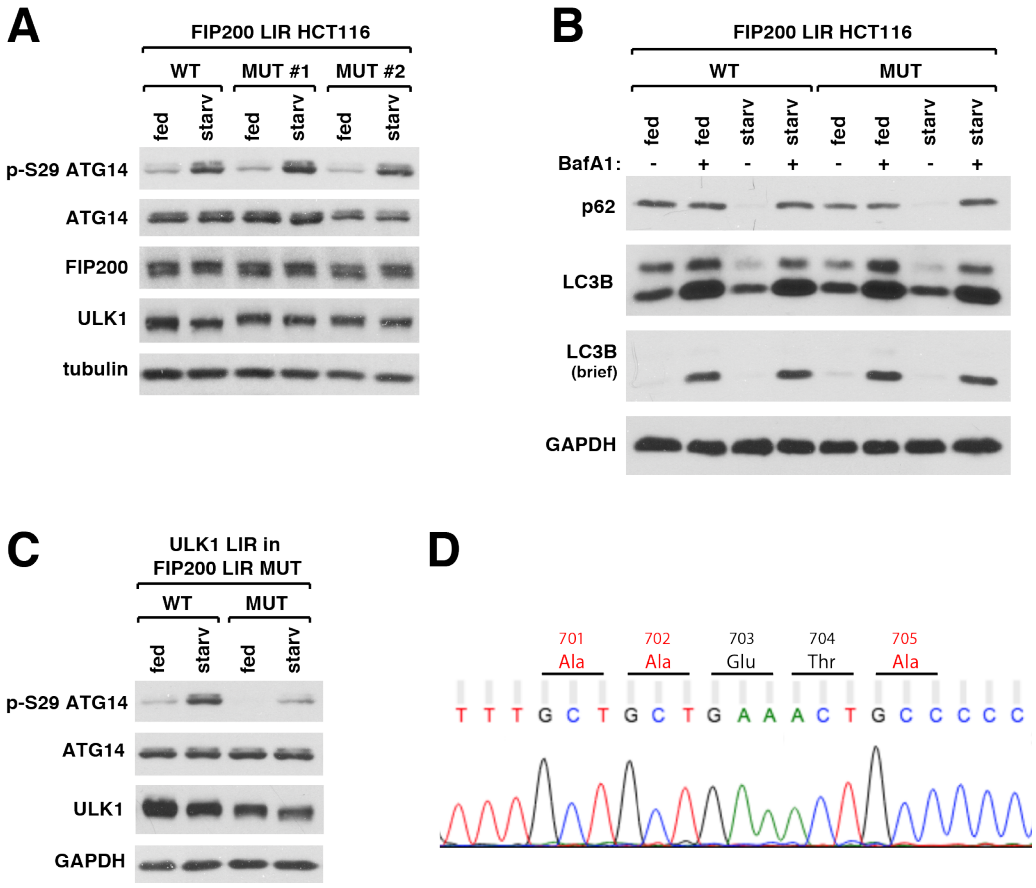
A
FIP200 LIR HCT116
WT
MUT #1
MUT #2
fed
starv
p-S29 ATG14
ATG14
FIP200
ULK1
tubulin
B
FIP200 LIR HCT116
WT
MUT
BafA1:
p62
LC3B
LC3B (brief)
GAPDH
C
ULK1 LIR in FIP200 LIR MUT
WT
MUT
p-S29 ATG14
ATG14
ULK1
GAPDH
D
701 Ala
702 Ala
703 Glu
704 Thr
705 Ala
T T T G C T G C T G A A A C T G C C C C C

Figure 27. ATG8 binding to FIP200 is not important for ULK1 activity or autophagy. (A) ATG8 binding to FIP200 does not regulate ULK1 activity. Wild type (WT) or FIP200 LIR mutant (MUT) HCT116 cells were cultured in full medium or EBSS for 60 min. Whole-cell extracts were collected and assessed for p-ATG14 by WB. Two independent FIP200 LIR mutant clones (MUT #1 and MUT#2) were tested. **(B)** Atg8 binding to FIP200 does not regulate the autophagic flux of SQSTM1 and LC3B. WT or FIP200 LIR mutant cells were cultured in full medium or EBSS for 2 h in the presence or absence of autophagy inhibitor bafilomycin A1 (BafA1) at 100nM. **(C)** ATG8 binding to FIP200 does not compensate for ATG8 binding to ULK1. WT or ULK1 LIR mutant (both in FIP200 LIR mutant background) HCT116 cells were cultured on full medium or starved with EBSS for 60 min. **(D)** Sequencing of FIP200 LIR for HCT116 cells confirms the mutation. The sequencing chromatogram shown was obtained from the sequencing provider, GENEWIZ, Inc. The ULK1 LIR mutation in the FIP200/ULK1 LIR mutant used in (C) was also confirmed by sequencing (data not shown).

4.6. Conclusion

The focus of this part of my study was on defining the function of the interaction between ATG8 proteins and the ULK1 complex. By mutating the LIR of endogenously expressed ULK1, and disrupting its interaction with ATG8 proteins, we have shown that ATG8 binding to ULK1 plays a positive role in the autophagic clearance of SQSTM1 and LC3B-II, markers commonly used to assay autophagy. Furthermore, we have shown that ATG8 binding to the ULK1 complex functions in the biogenesis of autophagosomes and isolation membranes, suggesting a role for the interaction in earlier autophagy events. Lastly, we found that the binding of ATG8 to ULK1 is essential for the formation of ULK1 puncta during autophagy and promotes ULK1 activity. This study is the first to demonstrate that ATG8 binding to the ULK1 complex plays a role in autophagy, marking an important step in understanding how ULK1 is regulated and mediates autophagy.

CHAPTER 5

DISCUSSION

5.1. The interaction between ATG8 proteins and the ULK1 complex

In Chapter 2, we compared the interaction between each ATG8 protein and endogenously expressed human ULK1 complex, and found that GABARAP proteins have greater affinity than LC3 proteins for the ULK1 complex. This finding is in agreement with a previous report that showed recombinant human ULK1 preferentially interacts with the GABARAP subfamily of ATG8 proteins [104]. This observation indicates that GABARAP proteins might have a specific role in regulating the ULK1 complex, or conversely, that the ULK1 complex might have a role in regulating GABARAP proteins.

Given that ULK1 is regulated by nutrient status [32–34], we suspected that the interaction between the ULK1 complex and GABARAP proteins might be regulated by starvation, acting as a trigger to regulate ULK1 function and autophagy. However, we found that the interaction between GABARAPs and the ULK1 complex was not drastically changed between the fed and starved condition (Figure 9A). This result indicates that the interaction might be constitutive and that the regulation of the ULK1-GABARAP interaction is not a mechanism to regulate autophagy. However, it is important to note here that our finding is based on co-immunoprecipitation experiments. It is possible that subtle changes in ULK1-GABARAP binding affinity occur in starved cells but were not preserved when cells were lysed with strong detergents. Therefore, we cannot rule out the possibility that this interaction is regulated by nutrient condition. Clarification on the regulation of the interaction requires further investigation and might require a different approach.

In addition to its strong interaction with GABARAP proteins, we showed that ATG13 interacted with LC3C. Moreover, LC3C interacted with the ULK1 complex that was expressed endogenously in human cells, implying that there might be a biological role of the LC3C-ULK1 complex interaction. Interestingly, of all the six ATG8 proteins tested, only LC3C showed a drastic change in affinity for the ULK1 complex during nutrient starvation. Whereas the other ATG8 proteins appear to bind the ULK1 complex constitutively, the enhanced binding observed with LC3C during starvation indicates that the LC3C-ULK1 complex interaction is regulated, and therefore might play a role in regulating autophagy.

Considering our limited knowledge on LC3C, it is difficult to discern how LC3C binding to the ULK1 complex might function. Relative to LC3B, LC3C is expressed at low levels in human cells and is localized throughout the cytoplasm and perinuclear region [62,114,115]. Similar to other ATG8 proteins, LC3C is conjugated with phosphatidylethanolamine and its expression in HeLa cells is increased by the autophagy inhibitor chloroquine, suggesting that endogenous LC3C is associated with autophagosomes and might have a role in autophagy [94]. Determining how LC3C interacts with ATG13 with a greater affinity than LC3A and LC3B and defining the role of the LC3C-ATG13 interaction will likely advance our understanding of how autophagy is regulated by the ULK1 complex.

Although we did not observe a striking difference in the binding of GABARAPs to the ULK1 complex during starvation, we did observe differences in binding when ATG7 was depleted. ATG7 is only known to function in ATG8 PE conjugation. Therefore, we attribute ATG7-dependent changes in the ULK1-ATG8 interaction to changes in PE conjugation of ATG8. Thus, it appears that PE conjugation of GABARAP and GABARAPL1 enhances their affinity for ULK1 (Figure 8). Given this result and that PE conjugation is induced by starvation, we would expect the ATG8-ULK1 interaction to be

enhanced by starvation, which we did not observe. It is possible that the starvation condition used not sufficient to induce enough PE-conjugation of the overexpressed recombinant ATG8 proteins to show a difference in co-immunoprecipitation. In that, there were changes in PE-conjugation of recombinant ATG8s between WT and ATG7 KO cells, but there were not changes in PE conjugation of recombinant ATG8 proteins between the fed and starved condition.

The enhance binding of PE conjugated GABARAPs to ULK1 might function to guide and stabilize the ULK1 complex at the autophagosomal membrane. This notion is supported by the observation that the LIR of recombinant ULK1 is important for its colocalization with GABARAP and GABARAPL1 at discrete puncta in cells, presumably autophagosomes [103,104].

Throughout this study we noticed variation between MYC-tagged ATG8 proteins in their immunoprecipitation efficiency. GABARAPL1 and GABARAPL2 were not as efficiently immunoprecipitated as GABARAP (Figure 5). MYC was fused to the N-terminus of each ATG8. It is possible that the folding of GABARAPL1 and GABARAPL2, or their interactions with other proteins, hindered anti-MYC antibody binding during the immunoprecipitation. It is also possible that the proteins might localize to a cellular compartment that is resistant to antibody access. Further biochemical analysis might be required to clarify the cause of the difference.

As one potential role of ATG8 binding to the ULK1 complex, we tested whether ATG8 binding affects the interaction between members of the ULK1 complex. Using recombinant LIR mutants of ULK1 or ATG13, we tested whether ATG8 binding to ULK1 or ATG13 affects the ULK1-ATG13 interaction. Clearly, binding of GABARAP to ULK1 or ATG13 was not required for the ULK1-ATG13 interaction (Figure 10). This

result was later corroborated in this study (Figure 24A) and is in agreement with a previous report that showed the LIR of Atg1 (yeast homolog of ULK1) is dispensable for its interaction with Atg13 [103].

5.2. Opposing roles of the ATG8 subfamilies in autophagy initiation

In addition to showing that the LC3 and GABARAP proteins have different affinities for the ULK1 complex, we showed that the two subfamilies have distinct roles in regulating the ULK1 complex and autophagy initiation. We found that the increase in WIPI2 puncta number in response to starvation was dampened in the GABARAP TKO HeLa cells, suggesting that the GABARAP subfamily positively regulates starvation-dependent isolation membrane biogenesis (Figure 15). Interestingly, in the fed state, GABARAP TKO cells show more WIPI2-positive puncta than wild type cells. This could suggest that GABARAPs either play a role in suppressing basal isolation membrane formation or play a role in the maturation or progression of autophagosomes. Alternatively, it is possible that a basal autophagy initiation pathway independent of ULK1 activity and GABARAPs exists and is upregulated with the loss of GABARAP proteins. Although a more thorough investigation is required to understand how GABARAP depletion results in more steady state isolation membranes, the possibility that GABARAPs suppress basal autophagy initiation seems unlikely, since basal autophagy activity is reduced in GABARAP-depleted cells [92,94]. Our finding corroborates a previous study that showed knockdown of the three GABARAP proteins resulted in the accumulation of Atg5-Atg16L puncta, which could be interpreted as stalled isolation membranes [92]. Early autophagosomal membrane markers such as WIPI2 and the ATG12-ATG5-ATG16L1 complex are not present on mature autophagosomes [116]. Therefore, it is possible that GABARAPs play a role in the release of those factors, which might be a critical step for autophagosome maturation. Thus, although GABARAPs are not absolutely required for isolation

membrane formation, they are important for their biogenesis during starvation and might also play a role in their progression.

We propose that the mechanism by which GABARAPs facilitate isolation membrane biogenesis is via their positive role in ULK1 activation. This is supported by our observation that the phosphorylation of several ULK1 substrates (ATG14 Ser29 and BECN1 Ser30) was reduced in GABARAP TKO Hela cells (Figure 12A). By reconstituting individual GABARAP proteins in GABARAP TKO HeLa cells, we determined that the role of promoting ULK1 activity is shared by GABARAP and GABARAPL1, as either protein was sufficient to restore ULK1 activity (Figure 13). The function of GABARAP and GABARAPL1 towards ULK1 activity is correlated with their relatively high affinity for ULK1 (shown in Chapter 2).

In agreement with our study and hypothesis that GABARAP proteins promote ULK1 activity, Joachim et al. reported that the knockdown of GABARAP alone in HEK293A cells reduced the phosphorylation of ATG13 at Ser355, a phosphorylation mediated by ULK1 that is important for mitophagy [106]. Although we found that complete depletion of GABARAP (KO) alone in HCT116 cells did not affect ULK1 activity and that GABARAPL1 expression, in the absence of GABARAP, was sufficient to restore ULK1 activity (Figure 13), it is possible that the contribution of GABARAP to ULK1 activity is specific to the cell type. We speculate that GABARAPL1 might not be expressed at sufficient levels to compensate for GABARAP deficiency in HEK293A cells.

It is unclear how GABARAP proteins promote ULK1 activity. A potential explanation comes from the observation that ULK1 protein expression was reduced in the GABARAP TKO and Hexa KO Hela cells. Therefore, it is possible that GABARAP proteins are promoting ULK1 substrate phosphorylation simply by promoting ULK1

expression. Indeed, re-expressing GABARAP and GABARAPL1 in the GABARAP TKO cells was sufficient to restore ULK1 expression along with p-ATG14 (Figure 13). However, even though it restored ULK1 expression, re-expressing GABARAPL2 did not restore p-ATG14. Thus, it appears that the mechanism by which GABARAPs promote ULK1 activity is not simply through mediating ULK1 expression. Understanding how GABARAP and GABARAPL1 promote ULK1 activity will require further investigation.

An intriguing finding in my study was that LC3-depleted cells showed an increase in the activity of ULK1 (Figure 12A). Through reconstitution analysis, we determined that LC3B and LC3C negatively regulate ULK1 activity. Our autophagy analysis indicates that LC3s are not required for autophagy activity. Therefore, it is possible that GABARAPs play a more prominent role than LC3s in autophagy. This notion is consistent with other reports [94,95]. In chapter 2, we found that the binding of LC3C to the ULK1 complex was enhanced during nutrient starvation. We speculate that the enhanced binding during nutrient starvation might function to curb ULK1 activity, preventing prolonged or hyper-activation of ULK1. Indeed, too much autophagy is deleterious for cells, and cells have evolved mechanisms to dampen ULK1 activity during starvation [48].

How the LC3 and GABARAP subfamilies have apparent opposing roles in regulating ULK1 activity is unclear. A clue for how the LC3 subfamily might suppress ULK1 comes from our finding that LC3-depleted cells have increased GABARAP protein expression (**Figure 12A**). It is possible that LC3 proteins suppress ULK1 activity by down-regulating the GABARAPs, ULK1 activators. Indeed, stably re-expressing LC3B or LC3C in LC3 TKO cells reduces protein expression of GABARAPs, which directly correlates with a reduction of ULK1 activity (**Figure 14A**). The role of LC3s acting as suppressors of ULK1 via GABARAP proteins is also supported by the result that the Hexa KO cells showed similar p-ATG14 levels to that of GABARAP TKO cells. If LC3s

were directly inhibiting ULK1 and acting independent of GABARAPs, one might expect ULK1 to have higher activity in the Hexa KO cells when compared to the GABARAP TKO cells.

Since LC3B does not interact with the ULK1 complex, it is likely that LC3B regulates ULK1 indirectly, possibly through down-regulating GABARAPs. However, we do not exclude a role of LC3C in directly regulating the ULK1 complex, as it showed a relatively strong binding affinity toward ATG13 (Figure 7A). It is unknown how LC3B and LC3C downregulate GABARAP expression, although it appears to be independent of autophagy since the LC3 TKO cells do not show a drastic defect in the basal or starvation-induced autophagic degradation of GABARAPL1 (**Figure 16**). Also, the effect of LC3B and LC3C on GABARAP protein expression is not correlated with a similar change in GABARAP mRNA expression, thus it appears that LC3B and LC3C are regulating GABARAP expression post-transcriptionally (**Figure 14B**). Further investigation is required to understand how LC3B and LC3C regulate the expression of GABARAP proteins.

5.3. ATG8 binding to ULK1 and ATG13 is important autophagy initiation

Multiple reports have shown that recombinant ULK1 interacts with ATG8 proteins and that this interaction is important for ULK1 to associate with autophagosomes [103–106]. However, whether this association is required for autophagy has been left unanswered. In this study, by introducing point mutations at the *ULK1* locus in human cells, we have shown that ATG8 binding to the ULK1 complex, expressed at endogenous levels, is important for ULK1 activation and the formation of isolation membranes and autophagosomes during starvation. These findings provide important insight into the mechanism by which the ULK1 complex mediates autophagy in response to starvation.

Lending to a mechanism for how GABARAPs mediate ULK1 activation (shown in Chapter 3), we found that the ULK1-mediated phosphorylations depend on the capacity of ATG8 proteins to physically interact with ULK1 (Figure 23). This finding implies that GABARAP proteins are promoting ULK1 activity by directly binding ULK1. In an attempt to understand how GABARAP binding to ULK1 promotes ULK1 activity, we addressed the possibility that post-translational modifications of ULK1 that mediate its activity might be regulated by its binding to ATG8. However, the phosphorylations of ULK1 by mTORC1 and AMPK were not drastically altered with the LIR mutant (Figure 23A). Thus, it appears that the mechanism by which ATG8 binding promotes ULK1 activity is not through mTORC1 or AMPK regulation of ULK1. As GABARAP proteins share structural homology with ubiquitin [67], it is also possible that GABARAPs are acting as post-translational modifications by binding to ULK1. This binding, or "modification", might induce a conformational change in ULK1, rendering it more active.

We have also considered the possibility that GABARAP proteins might promote ULK1 activity by binding to and stabilizing the ULK1 complex. Indeed, ubiquitination of ULK1 has been shown to affect ULK1 stability and function [47,48]. However, unlike in the GABARAP TKO or Hexa KO cells, ULK1 expression is not decreased in the ULK1 LIR mutant cells, indicating that ATG8 binding to ULK1 is not critical for ULK1 stability. This result, in addition to the results mentioned in Chapter 3, further supports the notion that GABARAPs are binding to and promoting ULK1 activity not simply by promoting ULK1 expression. However, as ATG8 binding to the ULK1 complex is not completely abolished in the ULK1 LIR mutant cells (Figure 25), we cannot exclude the possibility that GABARAPs may stabilize the ULK1 complex via their binding to ATG13.

In addition to showing that GABARAPs facilitate ULK1 activity and autophagy initiation by binding to ULK1, we showed evidence to suggest that the binding also regulates

autophagosome turnover. The number of steady state autophagosomes is greater in the ULK1 LIR mutant than in WT cells, and importantly, the mutant cells had less accumulation of autophagosomes when autophagosome-lysosome fusion was blocked with bafilomycin A1 (Figure 19). GABARAPs were shown to be critical for autophagosome-lysosome fusion [94], and perhaps, their role in fusion is dependent on their interaction with ULK1. This is a novel and important finding because to date, ULK1 does not have a defined role in autophagosome-lysosome fusion.

Similar to ULK1, we have shown that ATG8 binding to ATG13 positively regulates the ULK1-mediated phosphorylation of ATG14 at Ser29, suggesting that the ATG13-ATG8 interaction is also important for autophagy initiation. Interestingly, we found that ATG8 binding to FIP200 is dispensable for the phosphorylation of ATG14 and autophagy. How ATG8 binding to ULK1 and ATG13, but not FIP200, regulates autophagy is unclear. FIP200 binds to ATG8 protein *in vitro* [104], however it appears that FIP200 does not interact with ATG8 proteins when the proteins are expressed in human cells (Figure 6B). Although we observed endogenous FIP200 co-immunoprecipitated with ATG8 proteins expressed in HEK293T cells (Figure 5), the amount appeared to be reduced when compared to the amounts of co-immunoprecipitated ULK1 and ATG13, relative to the negative control. We suspect that the FIP200 co-precipitated might be indirect, through the ULK1-ATG8 and the ATG13-ATG8 interactions.

5.4. Final remarks and future perspectives

In corroboration of previous studies, our findings here support a role for ULK1 in mediating autophagy [32–34,36]. We have advanced our understanding of how ULK1 mediates autophagy by showing that ULK1 function depends on binding to ATG8 proteins. Furthermore, we have demonstrated that the role of ATG8 binding to ULK1 is to promote the phosphorylations of ULK1 substrates. Combining our findings here with

existing literature, we propose a model where ATG8 binding to ULK1 is important to activate ULK1 and mediate autophagy initiation (**Figure 28**). Considering our findings and a previous report that GABARAP proteins preferentially bind to ULK1 [104], GABARAP and GABARAPL1 are likely the ATG8 proteins that bind ULK1 to mediate autophagy initiation. Also, our evidence indicates that the PE conjugation of the GABARAPs is important for their binding to and activation of ULK1.

Defining specific roles of ATG8 proteins has been a recent subject of interest in the field of autophagy research. This study has contributed to our understanding of the functions of ATG8 proteins by showing that the GABARAP and LC3 subfamilies of ATG8 proteins have opposing roles in autophagy initiation through differentially regulating ULK1. While we have shown that GABARAP and GABARAPL1 likely mediate autophagy initiation by binding to and promoting ULK1 activity, it is less clear how the LC3 proteins suppress ULK1 activity. How the LC3 proteins downregulate GABARAP proteins remains unclear, and elucidating the interplay between the LC3 and GABARAP subfamilies will require further investigation.

The mechanism for how GABARAP proteins mediate autophagosome-lysosome fusion is unknown. By showing autophagosome turnover is reduced in ULK1 LIR mutant cells, our study hints at a possible role of the GABARAP-ULK1 complex interaction in autophagosome-lysosome fusion, and might contribute to defining how GABARAP proteins facilitate autophagosome-lysosome fusion.

FIGURE 28

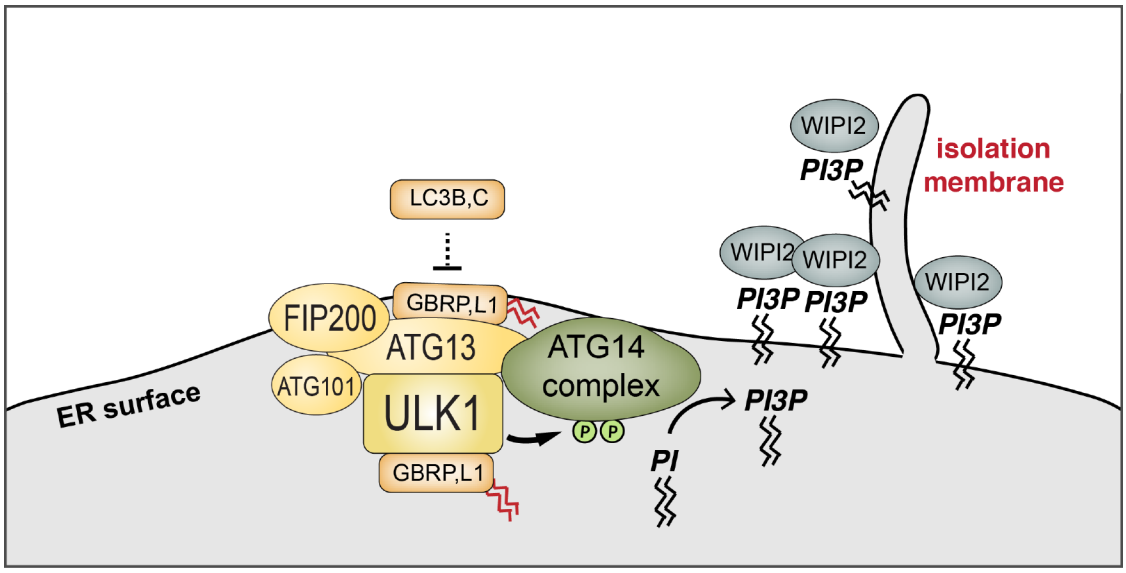

Figure 28. The role of ATG8 proteins in autophagy initiation. Full activation of ULK1 during nutrient starvation requires the binding of GABARAP and GABARAPL1 to ULK1 and ATG13, which at least partially depends on PE conjugation. Conjugation of GABARAPs with PE (shown in dark orange) increases their binding affinity for ULK1 and might stabilize the ULK1 complex at the ER and enhance ULK1 activity. LC3B and LC3C suppress ULK1 activation, possibly by down-regulating the protein expression of GABARAPs.

CHAPTER 6

MATERIALS AND METHODS

Antibodies and reagents. *The following primary antibodies were used in this study:* anti-ULK1 (sc-10900 for IP, sc-33182 for WB, sc-390904 for immunostaining), anti-SQSTM1 (sc-28359), anti-BECLIN 1 (sc-11427), anti-ATG14 for IP (sc-164767), anti-GAPDH (sc-25778), and anti-TUBULIN (sc-12462) from Santa Cruz Biotechnology; anti-ATG13 for IP (13468), anti-phospho-ATG14 Ser29 (13155), anti-phospho-ULK1 Ser757 (6888), anti-phospho-ULK1 Ser555 (5869), anti-ATG14 (96752), anti-GABARAPL1 (26632), anti-LC3A (4599), anti-LC3B (2775), anti-LC3C (14723), anti-ATG7 (8558) from Cell Signaling Technology; anti-MYC 9E10 (OP10) from EMD Biosciences; anti-HA (MMS-101P) from Biolegend; anti-GABARAPL2 (PM038), anti-LC3B for immunostaining (PM036) from MBL; anti-GABARAP (AP1821a) from Abgent; anti-phospho-ATG13 Ser318 (600-401-C49) from Rockland Immunochemicals Inc.; anti-FIP200 and anti-ATG13 for WB were generated as described previously [33]; anti-phospho-BECLIN Ser30 was generated as previously described [58].
The following reagents were used in this study: L-Glutamine (25030081), Penicillin-Streptomycin (15140122), Puromycin (A11138-03), and Zeocin (R250-01) from Thermo Fischer Scientific; bafilomycin A1 (B1793-10UG) and polybrene (H9268) from Sigma-Aldrich

Cell culture and transfection. HEK293T, HCT116, and HeLa cells were cultured at 37^{o}C in 5% CO_2 in full medium comprised of Dulbecco's Modified Eagle's Medium (DMEM; Thermo Fisher Scientific, 11995) supplemented with 10% fetal bovine serum (Thermo Fisher Scientific, 26140079), penicillin-streptomycin, and L-Glutamine. For transient expression, cells were transfected with recombinant DNA using Lipofectamine

3000 (Thermo Fisher Scientific, L3000075) following the manufacturer's protocol. Cell lysates were collected 48 h post-transfection. For nutrient starvation, full medium was replaced with Earle's Balanced Salt Solution (EBSS; MilliporeSigma; E2888), which contains no amino acids or serum.

Cell lysate preparation, immunoprecipitation, and western blotting. Cell lysates were prepared using lysis buffer containing 40 mM Hepes, pH 7.4, 120 mM NaCl, 1 mM EDTA, 50 mM NaF, 1.5 mM Na_3VO_4, 10 mM β-glycerophosphate, and 1% Triton X-100 (Sigma- Aldrich, T8787) supplemented with protease inhibitor cocktail (Roche Diagnostics, 11873580001). For immunoprecipitation experiments, cell lysates were incubated with protein G-agarose (GenDEPOT, P9202) and primary antibody at 4^{o}C for 3 h, followed by 4 washes with lysis buffer. Washed agarose containing immunoprecipitated protein (or just cell lysate for non-immunoprecipitation experiments) was incubated with sample buffer at 95^{o}C for 5 min. Denatured proteins were resolved by electrophoresis using 8%, 12%, or 4-12% Tris-glycine gels (Life Technologies). Proteins were transferred onto immunoblot polyvinylidene difluoride membranes (Bio-Rad, 1620177) and detected with ECL-based horseradish peroxidase substrate reagents (Advansta Inc., E-119-50).

For immunoprecipitation using DSP crosslinker: prior to collecting cell lysates, cells were incubated in PBS (phosphate buffered saline) with the indicated concentrations of DSP (dithiobis(succinimidyl propionate); 22586, Thermo Fischer Scientific) for 10 min. The DSP was then quenched by incubating cells in 40 mM Tris-HCl pH 7.4 for 10 min.

DNA constructs and ATG13 mutagenesis. Full-length cDNA for human ULK1, ATG13, FIP200, and all ATG8s were obtained from Open Biosystems, amplified by polymerase chain reaction (PCR), and cloned into the MYC or HA - pRK5 vector [117]. The ATG13 LIR mutation was made using a site-directed mutagenesis kit (Agilent

Technologies, 200522). Primers used to make the ATG13 LIR mutation and the ATG13 C-terminal deletion mutations are listed in **Table 1**. ATG13 LIR mutant and C-terminal deletion amplicons were cloned into the MYC-pRK5 vector.

TALEN-mediated knock out of ATG13 and GABARAPs. Transcription Activator-Like Effector Nucleases (TALEN) target sequences for ATG13, GABARAP, GABARAPL1, and GABARAPL2 were selected using TALEN-NT (https://tale-nt.cac.cornell.edu/) and are shown in **Table 2**. The oligonucleotides were assembled into pc_TALd152+63 using Golden Gate TALEN assembly [118]. HCT116 cells were transfected using the Neon Transfection System with 500 ng piggyBac 7 Transposase (PB7), 500 ng pPB-Ef1A-Puro transposon vector, and 2 μg of TALEN target sequence vector as previously described [119]. Three days post-transfection, cells were seeded into 96-well plates in full medium with puromycin at 1 μg/ml. Wells with two or more colonies were discarded. Single colonies were isolated, expanded, and screened for knockout by western blotting. *ATG13 KO cells were generated by Neil Otto of the Kim Lab.*

CRISPR-Cas9-mediated knock out of ATG7. The guide RNA (gRNA) sequence for ATG7 was selected using (http://crispr.mit/edu). The gRNA sequence fragment (5'-AGAAGAAGCTGAACGAGTAT-3') was cloned into the pSpCas9 (BB)-2A-GFP vector (Addgene). The vector DNA was introduced into HEK293T cells using the Neon Transfection System (Thermo Fisher Scientific, MPK5000). Two days post-transfection, single green fluorescent protein (GFP)-positive cells were plated per well of a 96-well dish using FACSAria II SORP (BD Biosciences). Single colonies were expanded and screened for knockout by western blotting using anti-ATG7 antibody. *ATG7 KO cells were generated by Daihyun Song of the Kim Lab.*

CRISPR-cas9-mediated mutation of ULK1 and FIP200 LIRs. gRNA sequences for ULK1 and FIP200 (5'- TGACACAGACGACTTCGTCA -3' and 5'- TATGTGCATCAATACTATC -3' respectively) were cloned into the pSpCas9 (BB)-2A-GFP vector. Replacement DNA encoding the ULK1 LIR mutation or FIP200 LIR mutation was synthesized by GenScript USA Inc. The CRISPR-cas9 vector and replacement DNA were introduced into HCT116 or HEK293T cells using the Neon Transfection System. Single GFP-positive colonies were isolated (as described above), and genomic DNA was extracted for mutation verification. In brief, cell pellets were resuspended in 50 mM NaOH and incubated at 95^{o}C for 30 min. After being neutralized with 1 M Tris-HCl, the cell extract was centrifuged at 15,200 x g for 10 min at 4^{o}C. The supernatant, containing genomic DNA, was used for PCR with primers listed in **Table 3**. Primers pairs were designed to anneal to wild type or mutant LIR DNA sequence. Clones only yielding a product with the mutant primers were considered to be potential homozygous mutants and were then analyzed by DNA sequencing to confirm the mutation. The region including the LIR was amplified using primers listed in **Table 3** and cloned into the pRK5 vector. The pRK5 insert was sequenced by GENEWIZ, Inc.

Preparation of stably reconstituted cells. *For stable expression in LC3 and GABARAP TKO HeLa cells:* Individual LC3 and GABARAP cDNAs were cloned into the lentiviral expression vector pCSII-EF-MCS, which was kindly provided by N. Somia (University of Minnesota, MN, USA). The vector was introduced into HEK293FT cells with lentiviral packaging vectors, DNRF-HIV-1-gag-pol (provided by N. Somia) and pCMV-VSV-G (provided by S. Stewart at the Washington University, St Louis, MO), using Lipofectamine 3000. Medium that contained virus was collected 60 h post-transduction. Cell debris from the viral soup was removed using a 0.45-mm filter. One million cells per 6-cm dish were incubated with the collected virus twice in the presence of polybrene at 8

μg/ml. The first infection was performed using 1.5 ml of viral soup for 4 h. The second infection was performed overnight using 0.5 ml of viral soup combined with 3.5 ml of full medium. 48 h after the second infection, medium was replaced with full medium with zeocin at 100 μg/ml.

For stable expression in ATG13 KO HCT116 cells: MYC-tagged ATG13 WT, LIR mutant, or empty cDNAs were cloned into pCSII-EF-MCS. The same procedure as described above was followed, except that ATG13 KO HCT116 cells were transduced. *Stably reconstituted ATG13 KO cells were generated by Neil Otto of the Kim Lab.*

Immunofluorescence microscopy. Cells were cultured on glass coverslips, fixed with 4% formaldehyde in PBS for 15 min, and permeabilized with 0.25% Triton X-100 (Sigma, T8787) for 5 min at room temperature. Permeabilized cells were incubated in PBST (PBS with 0.05% Tween) containing 2% Bovine Serum Albumin (Calbiochem) for 60 min and then incubated with primary antibodies overnight at 4°C. After the primary antibody labeling, cells were incubated with Alexa Flour 488-conjugated anti-rabbit IgG (A-21441, Invitrogen) or Alexa Flour 555- conjugated anti-mouse IgG (A-31570, Invitrogen). Nuclei were stained with DAPI (4'-6- diamidino-2-phenylindole; Invitrogen, D-1306). Cell images were obtained using a Deltavision PersonelDV microscope (Applied Precision). Puncta were quantified using ImageJ and statistically analyzed by Student t- test using the Prism v6 software (GraphPad Software Inc, La Jolla, CA, USA).

mRNA analysis by qRT-PCR. Total RNA was isolated using TRIzol Reagent (Thermo Fischer Scientific, 15596018) and cDNA was synthesized using a reverse transcriptase kit (GenDEPOT, R5600) following the manufacturers' protocols. Quantitative reverse transcription (qRT)-PCR was performed using SYBR Green Supermix (Bio-Rad) and a Bio-Rad CFX 96 real-time system. Primers used in the reaction are listed in **Table 4.** The

CT value for each GABARAP target mRNA was normalized to the corresponding GAPDH mRNA.

Statistical analysis. Western blot protein bands were quantitatively analyzed for their intensities using ImageJ software. Cell images were quantitatively analyzed by counting the number of puncta in each cell, setting the same threshold for control and experimental groups using ImageJ. Outcomes were summarized by using the mean and the standard error of the mean (SEM) as indicated in the figure legends. Statistical significance of difference between groups was analyzed by the Student t test using Prism 6 (Version 6.0d, GraphPad Software).

TABLES

Table 1. Primers for ATG13 mutagenesis

ATG13 LIR *FWD*: GACTTTGTTATGGCGGCGTTTAAACCAGCT
ATG13 LIR *REV*: AGCTGGTTTAAACGCCGCCATAACAAAGTC

ATG13 (1-440) *FWD*: GAGCGAGTCGACATGGAAACTGATCTCAAT
ATG13 (1-440) *REV*: GTCTCGAAGCGGCCGCTTAGGTATTGCCACTGCTGCC

ATG13 (1-452) *FWD*: GAGCGAGTCGACATGGAAACTGATCTCAAT
ATG13 (1-452) *REV*: GTCTCGAAGCGGCCGCTTAAGCTGGTTTAAAGTCTAT

ATG13 (1-510) *FWD*: GAGCGAGTCGACATGGAAACTGATCTCAAT
ATG13 (1-510) *REV*: GTCTCGAAGCGGCCGCTTAATCAAACTCGCGGACATT

Table 2. TALEN target sequences to generate KO cells

GABARAP: TGTCCAGCCCGGTTCCCgggaggatgaagttCGTGTACAAAGAAGAGCA
GABARAPL1: TGCATCATGAAGTTCCAgtacaaggaggaccaTCCCTTTGAGTATCGGAAA
GABARAPL2: TTCCGTCCCCTTCCCGCCGccgccatgaagtggATGTTCAAGGAGGACCA
ATG13: TCCCTTCTTGCTATAActagggtgacaccagCCTATAGGCTCTCCAGGA

Table 3. Primers to confirm LIR mutations

Genotyping to screen LIR mutations

ULK1 LIR WT *FWD*: CTGTGACACAGACGACTTCG
ULK1 LIR WT *REV*: CCCATCCTAACTGCCCATAA

ULK1 LIR MUT *FWD*: CTGTGACACAGACGCAGC
ULK1 LIR MUT *REV*: CCCATCCTAACTGCCCATAA

FIP200 LIR WT *FWD*: CGTTTGATTTTGAAACTATTCCC
FIP200 LIR WT *REV*: ACCATCATTTCTGGGCTTTG

FIP200 LIR MUT *FWD*: GTTTGCTGCTGAAACTGCC
FIP200 LIR MUT *REV*: ACCATCATTTCTGGGCTTTG

LIR amplification to clone into pRK5 for sequencing

ULK1 LIR *FWD*: GAGCGAGTCGACCAATTTGCTCCCCTGAGTGTG
ULK1 LIR *REV*: GTCTCGAAGCGGCCGCCCCATCCTAACTGCCCATAA

FIP200 LIR *FWD*: GAGCGAGTCGACTCCAGGCATCTGTGAGTCAG
FIP200 LIR *REV*: GTCTCGAAGCGGCCGCATCATTTCTGGGCTTTGTGG

Table 4. qRT-PCR primers used for mRNA analysis of GABARAPs

GABARAP *FWD*: GGGTGCCGGTGATAGTAGAA
GABARAP *REV*: AATTCGCTTCCGGATCAAG

GABARAPL1 *FWD*: GGTCCCCGTGATTGTAGAGA
GABARAPL1 *REV*: GTCCTCAGGTCTCAGGTGGA

GABARAPL2 *FWD*: CCGTCGTTGTTGTTGTGCT
GABARAPL2 *REV*: CATCTGTGTTCCAGCGAGTG

GAPDH *FWD*: GAGTCAACGGATTTGGTCGT
GAPDH *REV*: TGGGTGGAATCATATTGGAA

Bibliography

1. Shibata, M. *et al.* Regulation of Intracellular Accumulation of Mutant Huntingtin by Beclin 1. *J. Biol. Chem.* **281,** 14474–14485 (2006).
2. Webb, J. L., Ravikumar, B., Atkins, J., Skepper, J. N. & Rubinsztein, D. C. α-Synuclein Is Degraded by Both Autophagy and the Proteasome. *J. Biol. Chem.* **278,** 25009–25013 (2003).
3. Ravikumar, B., Duden, R. & Rubinsztein, D. C. Aggregate-prone proteins with polyglutamine and polyalanine expansions are degraded by autophagy. *Hum. Mol. Genet.* **11,** 1107–17 (2002).
4. Singh, R. *et al.* Autophagy regulates lipid metabolism. *Nature* **458,** 1131–1135 (2009).
5. Kudchodkar, S. B. & Levine, B. Viruses and autophagy. *Rev. Med. Virol.* **19,** 359–78 (2009).
6. Levine, B. Eating Oneself and Uninvited Guests. *Cell* **120,** 159–162 (2005).
7. Youle, R. J. & Narendra, D. P. Mechanisms of mitophagy. *Nat. Rev. Mol. Cell Biol.* **12,** 9–14 (2011).
8. Ashrafi, G., Schlehe, J. S., LaVoie, M. J. & Schwarz, T. L. Mitophagy of damaged mitochondria occurs locally in distal neuronal axons and requires PINK1 and Parkin. *J. Cell Biol.* **206,** 655–70 (2014).
9. Taylor, J. P., Hardy, J. & Fischbeck, K. H. Toxic Proteins in Neurodegenerative Disease. *Science (80-.).* **296,** 1991–1995 (2002).
10. Perutz, M. F. & Windle, A. H. Cause of neural death in neurodegenerative diseases attributable to expansion of glutamine repeats. *Nature* **412,** 143–144 (2001).
11. Sánchez, I., Mahlke, C. & Yuan, J. Pivotal role of oligomerization in expanded polyglutamine neurodegenerative disorders. *Nature* **421,** 373–379 (2003).
12. Ballinger, S. W. Mitochondrial dysfunction in cardiovascular disease. *Free Radic. Biol. Med.* **38,** 1278–1295 (2005).
13. Perera, R. M. *et al.* Transcriptional control of autophagy–lysosome function drives pancreatic cancer metabolism. *Nature* **524,** 361–365 (2015).
14. Hu, Y.-L., Jahangiri, A., DeLay, M. & Aghi, M. K. Tumor Cell Autophagy as an Adaptive Response Mediating Resistance to Treatments Such as Antiangiogenic Therapy. *Cancer Res.* **72,** 4294–4299 (2012).
15. Guo, J. Y. *et al.* Activated Ras requires autophagy to maintain oxidative metabolism and tumorigenesis. *Genes Dev.* **25,** 460–470 (2011).
16. Yang, S. *et al.* Pancreatic cancers require autophagy for tumor growth. *Genes Dev.* **25,** 717–729 (2011).
17. Rao, S. *et al.* A dual role for autophagy in a murine model of lung cancer. *Nat. Commun.* **5,** 3056 (2014).
18. Shingu, T. *et al.* Inhibition of autophagy at a late stage enhances imatinib-induced cytotoxicity in human malignant glioma cells. *Int. J. Cancer* **124,** 1060–1071 (2009).
19. Liu, D., Yang, Y., Liu, Q. & Wang, J. Inhibition of autophagy by 3-MA potentiates cisplatin-induced apoptosis in esophageal squamous cell carcinoma cells. *Med. Oncol.* **28,** 105–111 (2011).
20. Apel, A., Herr, I., Schwarz, H., Rodemann, H. P. & Mayer, A. Blocked Autophagy

Sensitizes Resistant Carcinoma Cells to Radiation Therapy. *Cancer Res.* **68,** 1485–1494 (2008).
21. Dikic, I. & Elazar, Z. Mechanism and medical implications of mammalian autophagy. *Nat. Rev. Mol. Cell Biol.* **19,** 349–364 (2018).
22. Nair, U. *et al.* SNARE Proteins Are Required for Macroautophagy. *Cell* **146,** 290–302 (2011).
23. Ravikumar, B., Moreau, K., Jahreiss, L., Puri, C. & Rubinsztein, D. C. Plasma membrane contributes to the formation of pre-autophagosomal structures. *Nat. Cell Biol.* **12,** 747–757 (2010).
24. Hailey, D. W. *et al.* Mitochondria Supply Membranes for Autophagosome Biogenesis during Starvation. *Cell* **141,** 656–667 (2010).
25. DE DUVE, C. The lysosome. *Sci. Am.* **208,** 64–72 (1963).
26. Thumm, M. *et al.* Isolation of autophagocytosis mutants of Saccharomyces cerevisiae. *FEBS Lett.* **349,** 275–80 (1994).
27. Tsukada, M. & Ohsumi, Y. Isolation and characterization of autophagy-defective mutants of Saccharomyces cerevisiae. *FEBS Lett.* **333,** 169–74 (1993).
28. Kroemer, G., Mariño, G. & Levine, B. Autophagy and the integrated stress response. *Mol. Cell* **40,** 280–93 (2010).
29. Mercer, C. A., Kaliappan, A. & Dennis, P. B. A novel, human Atg13 binding protein, Atg101, interacts with ULK1 and is essential for macroautophagy. *Autophagy* **5,** 649–62 (2009).
30. Hosokawa, N. *et al.* Atg101, a novel mammalian autophagy protein interacting with Atg13. *Autophagy* **5,** 973–9 (2009).
31. Chang, Y.-Y. & Neufeld, T. P. An Atg1/Atg13 Complex with Multiple Roles in TOR-mediated Autophagy Regulation. *Mol. Biol. Cell* **20,** 2004–2014 (2009).
32. Ganley, I. G. *et al.* ULK1·ATG13·FIP200 Complex Mediates mTOR Signaling and Is Essential for Autophagy. *J. Biol. Chem.* **284,** 12297–12305 (2009).
33. Jung, C. H. *et al.* ULK-Atg13-FIP200 Complexes Mediate mTOR Signaling to the Autophagy Machinery. *Mol. Biol. Cell* **20,** 1992–2003 (2009).
34. Hosokawa, N. *et al.* Nutrient-dependent mTORC1 Association with the ULK1–Atg13–FIP200 Complex Required for Autophagy. *Mol. Biol. Cell* **20,** 1981–1991 (2009).
35. Hara, T. *et al.* FIP200, a ULK-interacting protein, is required for autophagosome formation in mammalian cells. *J. Cell Biol.* **181,** 497–510 (2008).
36. Chan, E. Y. W., Kir, S. & Tooze, S. A. siRNA Screening of the Kinome Identifies ULK1 as a Multidomain Modulator of Autophagy. *J. Biol. Chem.* **282,** 25464–25474 (2007).
37. Wong, P.-M., Feng, Y., Wang, J., Shi, R. & Jiang, X. Regulation of autophagy by coordinated action of mTORC1 and protein phosphatase 2A. *Nat. Commun.* **6,** 8048 (2015).
38. Itakura, E. & Mizushima, N. Characterization of autophagosome formation site by a hierarchical analysis of mammalian Atg proteins. *Autophagy* **6,** 764–76 (2010).
39. Nishimura, T. *et al.* Autophagosome formation is initiated at phosphatidylinositol synthase-enriched ER subdomains. *EMBO J.* **36,** 1719–1735 (2017).
40. Egan, D. F. *et al.* Small Molecule Inhibition of the Autophagy Kinase ULK1 and Identification of ULK1 Substrates. *Mol. Cell* **59,** 285–297 (2015).

41. Puente, C., Hendrickson, R. C. & Jiang, X. Nutrient-regulated Phosphorylation of ATG13 Inhibits Starvation-induced Autophagy. *J. Biol. Chem.* **291,** 6026–6035 (2016).
42. Lee, J. W., Park, S., Takahashi, Y. & Wang, H.-G. The Association of AMPK with ULK1 Regulates Autophagy. *PLoS One* **5,** e15394 (2010).
43. Kim, J., Kundu, M., Viollet, B. & Guan, K.-L. AMPK and mTOR regulate autophagy through direct phosphorylation of Ulk1. *Nat. Cell Biol.* **13,** 132–141 (2011).
44. Egan, D. F. *et al.* Phosphorylation of ULK1 (hATG1) by AMP-Activated Protein Kinase Connects Energy Sensing to Mitophagy. *Science (80-.).* **331,** 456–461 (2011).
45. Gwinn, D. M. *et al.* AMPK Phosphorylation of Raptor Mediates a Metabolic Checkpoint. *Mol. Cell* **30,** 214–226 (2008).
46. Lin, S.-Y. *et al.* GSK3-TIP60-ULK1 Signaling Pathway Links Growth Factor Deprivation to Autophagy. *Science (80-.).* **336,** 477–481 (2012).
47. Nazio, F. *et al.* mTOR inhibits autophagy by controlling ULK1 ubiquitylation, self-association and function through AMBRA1 and TRAF6. *Nat. Cell Biol.* **15,** 406–416 (2013).
48. Liu, C.-C. *et al.* Cul3-KLHL20 Ubiquitin Ligase Governs the Turnover of ULK1 and VPS34 Complexes to Control Autophagy Termination. *Mol. Cell* **61,** 84–97 (2016).
49. Roberts, R. & Ktistakis, N. T. Omegasomes: PI3P platforms that manufacture autophagosomes. *Essays Biochem.* **55,** 17–27 (2013).
50. Matsunaga, K. *et al.* Autophagy requires endoplasmic reticulum targeting of the PI3-kinase complex via Atg14L. *J. Cell Biol.* **190,** 511–521 (2010).
51. Fan, W., Nassiri, A. & Zhong, Q. Autophagosome targeting and membrane curvature sensing by Barkor/Atg14(L). *Proc. Natl. Acad. Sci.* **108,** 7769–7774 (2011).
52. Sun, Q. *et al.* Identification of Barkor as a mammalian autophagy-specific factor for Beclin 1 and class III phosphatidylinositol 3-kinase. *Proc. Natl. Acad. Sci.* **105,** 19211–19216 (2008).
53. Itakura, E., Kishi, C., Inoue, K. & Mizushima, N. Beclin 1 Forms Two Distinct Phosphatidylinositol 3-Kinase Complexes with Mammalian Atg14 and UVRAG. *Mol. Biol. Cell* **19,** 5360–5372 (2008).
54. Zhong, Y. *et al.* Distinct regulation of autophagic activity by Atg14L and Rubicon associated with Beclin 1–phosphatidylinositol-3-kinase complex. *Nat. Cell Biol.* **11,** 468–476 (2009).
55. Matsunaga, K. *et al.* Two Beclin 1-binding proteins, Atg14L and Rubicon, reciprocally regulate autophagy at different stages. *Nat. Cell Biol.* **11,** 385–396 (2009).
56. Di Bartolomeo, S. *et al.* The dynamic interaction of AMBRA1 with the dynein motor complex regulates mammalian autophagy. *J. Cell Biol.* **191,** 155–168 (2010).
57. Russell, R. C. *et al.* ULK1 induces autophagy by phosphorylating Beclin-1 and activating VPS34 lipid kinase. *Nat. Cell Biol.* **15,** 741–750 (2013).
58. Park, J.-M. *et al.* ULK1 phosphorylates Ser30 of BECN1 in association with

ATG14 to stimulate autophagy induction. *Autophagy* **14,** 584–597 (2018).
59. Park, J.-M. *et al.* The ULK1 complex mediates MTORC1 signaling to the autophagy initiation machinery via binding and phosphorylating ATG14. *Autophagy* **12,** 547–564 (2016).
60. Axe, E. L. *et al.* Autophagosome formation from membrane compartments enriched in phosphatidylinositol 3-phosphate and dynamically connected to the endoplasmic reticulum. *J. Cell Biol.* **182,** 685–701 (2008).
61. Polson, H. E. J. *et al.* Mammalian Atg18 (WIPI2) localizes to omegasome-anchored phagophores and positively regulates LC3 lipidation. *Autophagy* **6,** 506–522 (2010).
62. He, H. *et al.* Post-translational Modifications of Three Members of the Human MAP1LC3 Family and Detection of a Novel Type of Modification for MAP1LC3B. *J. Biol. Chem.* **278,** 29278–29287 (2003).
63. Ichimura, Y. *et al.* A ubiquitin-like system mediates protein lipidation. *Nature* **408,** 488–492 (2000).
64. Sugawara, K. *et al.* The crystal structure of microtubule-associated protein light chain 3, a mammalian homologue of Saccharomyces cerevisiae Atg8. *Genes to Cells* **9,** 611–618 (2004).
65. Tanida, I., Ueno, T. & Kominami, E. Human Light Chain 3/MAP1LC3B Is Cleaved at Its Carboxyl-terminal Met ^{121} to Expose Gly ^{120} for Lipidation and Targeting to Autophagosomal Membranes. *J. Biol. Chem.* **279,** 47704–47710 (2004).
66. Fujita, N. *et al.* An Atg4B Mutant Hampers the Lipidation of LC3 Paralogues and Causes Defects in Autophagosome Closure. *Mol. Biol. Cell* **19,** 4651–4659 (2008).
67. Bavro, V. N. *et al.* Crystal structure of the GABA(A)-receptor-associated protein, GABARAP. *EMBO Rep.* **3,** 183–9 (2002).
68. Mizushima, N. *et al.* Dissection of autophagosome formation using Apg5-deficient mouse embryonic stem cells. *J. Cell Biol.* **152,** 657–68 (2001).
69. Hanada, T. *et al.* The Atg12-Atg5 Conjugate Has a Novel E3-like Activity for Protein Lipidation in Autophagy. *J. Biol. Chem.* **282,** 37298–37302 (2007).
70. Suzuki, K. *et al.* The pre-autophagosomal structure organized by concerted functions of APG genes is essential for autophagosome formation. *EMBO J.* **20,** 5971–81 (2001).
71. Nakatogawa, H., Ichimura, Y. & Ohsumi, Y. Atg8, a Ubiquitin-like Protein Required for Autophagosome Formation, Mediates Membrane Tethering and Hemifusion. *Cell* **130,** 165–178 (2007).
72. Knorr, R. L. *et al.* Membrane Morphology Is Actively Transformed by Covalent Binding of the Protein Atg8 to PE-Lipids. *PLoS One* **9,** e115357 (2014).
73. Ichimura, Y. *et al.* In vivo and in vitro reconstitution of Atg8 conjugation essential for autophagy. *J. Biol. Chem.* **279,** 40584–92 (2004).
74. Dooley, H. C. *et al.* WIPI2 Links LC3 Conjugation with PI3P, Autophagosome Formation, and Pathogen Clearance by Recruiting Atg12–5-16L1. *Mol. Cell* **55,** 238–252 (2014).
75. Fujita, N. *et al.* The Atg16L Complex Specifies the Site of LC3 Lipidation for Membrane Biogenesis in Autophagy. *Mol. Biol. Cell* **19,** 2092–2100 (2008).
76. Nishimura, T. *et al.* FIP200 regulates targeting of Atg16L1 to the isolation

membrane. *EMBO Rep.* **14,** 284–291 (2013).
77. Mari, M. *et al.* An Atg9-containing compartment that functions in the early steps of autophagosome biogenesis. *J. Cell Biol.* **190,** 1005–1022 (2010).
78. Yamamoto, H. *et al.* Atg9 vesicles are an important membrane source during early steps of autophagosome formation. *J. Cell Biol.* **198,** 219–233 (2012).
79. Orsi, A. *et al.* Dynamic and transient interactions of Atg9 with autophagosomes, but not membrane integration, are required for autophagy. *Mol. Biol. Cell* **23,** 1860–73 (2012).
80. Puri, C., Renna, M., Bento, C. F., Moreau, K. & Rubinsztein, D. C. Diverse Autophagosome Membrane Sources Coalesce in Recycling Endosomes. *Cell* **154,** 1285–1299 (2013).
81. Zhou, C. *et al.* Regulation of mATG9 trafficking by Src- and ULK1-mediated phosphorylation in basal and starvation-induced autophagy. *Cell Res.* **27,** 184–201 (2017).
82. Papinski, D. *et al.* Early Steps in Autophagy Depend on Direct Phosphorylation of Atg9 by the Atg1 Kinase. *Mol. Cell* **53,** 471–483 (2014).
83. Young, A. R. J. *et al.* Starvation and ULK1-dependent cycling of mammalian Atg9 between the TGN and endosomes. *J. Cell Sci.* **119,** 3888–3900 (2006).
84. Lystad, A. H. *et al.* Structural determinants in GABARAP required for the selective binding and recruitment of ALFY to LC3B-positive structures. *EMBO Rep.* **15,** 557–65 (2014).
85. Shpilka, T., Weidberg, H., Pietrokovski, S. & Elazar, Z. Atg8: an autophagy-related ubiquitin-like protein family. *Genome Biol.* **12,** 226 (2011).
86. Rogov, V., Dötsch, V., Johansen, T. & Kirkin, V. Interactions between Autophagy Receptors and Ubiquitin-like Proteins Form the Molecular Basis for Selective Autophagy. *Mol. Cell* **53,** 167–178 (2014).
87. Kabeya, Y. *et al.* LC3, GABARAP and GATE16 localize to autophagosomal membrane depending on form-II formation. *J. Cell Sci.* **117,** 2805–2812 (2004).
88. Koukourakis, M. I. *et al.* Autophagosome Proteins LC3A, LC3B and LC3C Have Distinct Subcellular Distribution Kinetics and Expression in Cancer Cell Lines. *PLoS One* **10,** e0137675 (2015).
89. Landajuela, A. *et al.* Lipid Geometry and Bilayer Curvature Modulate LC3/GABARAP-Mediated Model Autophagosomal Elongation. *Biophys. J.* **110,** 411–422 (2016).
90. McEwan, D. G. *et al.* PLEKHM1 Regulates Autophagosome-Lysosome Fusion through HOPS Complex and LC3/GABARAP Proteins. *Mol. Cell* **57,** 39–54 (2015).
91. Albanesi, J., Wang, H., Sun, H.-Q., Levine, B. & Yin, H. GABARAP-mediated targeting of PI4K2A/PI4KIIα to autophagosomes regulates PtdIns4P-dependent autophagosome-lysosome fusion. *Autophagy* **11,** 2127–2129 (2015).
92. Weidberg, H. *et al.* LC3 and GATE-16/GABARAP subfamilies are both essential yet act differently in autophagosome biogenesis. *EMBO J.* **29,** 1792–1802 (2010).
93. Weidberg, H. *et al.* LC3 and GATE-16 N Termini Mediate Membrane Fusion Processes Required for Autophagosome Biogenesis. *Dev. Cell* **20,** 444–454 (2011).
94. Nguyen, T. N. *et al.* Atg8 family LC3/GABARAP proteins are crucial for

autophagosome-lysosome fusion but not autophagosome formation during PINK1/Parkin mitophagy and starvation. *J. Cell Biol.* **215,** 857–874 (2016).
95. Engedal, N. & Seglen, P. O. Autophagy of cytoplasmic bulk cargo does not require LC3. *Autophagy* **12,** 439–41 (2016).
96. Birgisdottir, Å. B., Lamark, T. & Johansen, T. The LIR motif - crucial for selective autophagy. *J. Cell Sci.* **126,** 3237–47 (2013).
97. Noda, N. N. *et al.* Structural basis of target recognition by Atg8/LC3 during selective autophagy. *Genes to Cells* **13,** 1211–1218 (2008).
98. Ichimura, Y. *et al.* Structural Basis for Sorting Mechanism of p62 in Selective Autophagy. *J. Biol. Chem.* **283,** 22847–22857 (2008).
99. Kirkin, V. *et al.* A Role for NBR1 in Autophagosomal Degradation of Ubiquitinated Substrates. *Mol. Cell* **33,** 505–516 (2009).
100. Pankiv, S. *et al.* p62/SQSTM1 Binds Directly to Atg8/LC3 to Facilitate Degradation of Ubiquitinated Protein Aggregates by Autophagy. *J. Biol. Chem.* **282,** 24131–24145 (2007).
101. Bjørkøy, G. *et al.* p62/SQSTM1 forms protein aggregates degraded by autophagy and has a protective effect on huntingtin-induced cell death. *J. Cell Biol.* **171,** 603–614 (2005).
102. Novak, I. *et al.* Nix is a selective autophagy receptor for mitochondrial clearance. *EMBO Rep.* **11,** 45–51 (2010).
103. Kraft, C. *et al.* Binding of the Atg1/ULK1 kinase to the ubiquitin-like protein Atg8 regulates autophagy. *EMBO J.* **31,** 3691–3703 (2012).
104. Alemu, E. A. *et al.* ATG8 Family Proteins Act as Scaffolds for Assembly of the ULK Complex. *J. Biol. Chem.* **287,** 39275–39290 (2012).
105. Okazaki, N. *et al.* Interaction of the Unc-51-like kinase and microtubule-associated protein light chain 3 related proteins in the brain: possible role of vesicular transport in axonal elongation. *Brain Res. Mol. Brain Res.* **85,** 1–12 (2000).
106. Joachim, J. *et al.* Activation of ULK Kinase and Autophagy by GABARAP Trafficking from the Centrosome Is Regulated by WAC and GM130. *Mol. Cell* **60,** 899–913 (2015).
107. Joo, J. H. *et al.* Hsp90-Cdc37 Chaperone Complex Regulates Ulk1- and Atg13-Mediated Mitophagy. *Mol. Cell* **43,** 572–585 (2011).
108. Thomas, P. & Smart, T. G. HEK293 cell line: A vehicle for the expression of recombinant proteins. *J. Pharmacol. Toxicol. Methods* **51,** 187–200 (2005).
109. Komatsu, M. *et al.* Impairment of starvation-induced and constitutive autophagy in Atg7-deficient mice. *J. Cell Biol.* **169,** 425–34 (2005).
110. Lengauer, C., Kinzler, K. W. & Vogelstein, B. DNA methylation and genetic instability in colorectal cancer cells. *Proc. Natl. Acad. Sci. U. S. A.* **94,** 2545–50 (1997).
111. Bennett, S. E., Umar, A., Oshima, J., Monnat, R. J. & Kunkel, T. A. Mismatch repair in extracts of Werner syndrome cell lines. *Cancer Res.* **57,** 2956–60 (1997).
112. Elliott, B. & Jasin, M. Repair of double-strand breaks by homologous recombination in mismatch repair-defective mammalian cells. *Mol. Cell. Biol.* **21,** 2671–82 (2001).
113. Yamamoto, A. *et al.* Bafilomycin A1 prevents maturation of autophagic vacuoles by inhibiting fusion between autophagosomes and lysosomes in rat hepatoma cell

line, H-4-II-E cells. *Cell Struct. Funct.* **23,** 33–42 (1998).
114. Xin, Y. *et al.* Cloning, Expression Patterns, and Chromosome Localization of Three Human and Two Mouse Homologues of GABAA Receptor-Associated Protein. *Genomics* **74,** 408–413 (2001).
115. Koukourakis, M. I. *et al.* Autophagosome Proteins LC3A, LC3B and LC3C Have Distinct Subcellular Distribution Kinetics and Expression in Cancer Cell Lines. *PLoS One* **10,** e0137675 (2015).
116. Nair, U., Cao, Y., Xie, Z. & Klionsky, D. J. Roles of the Lipid-binding Motifs of Atg18 and Atg21 in the Cytoplasm to Vacuole Targeting Pathway and Autophagy. *J. Biol. Chem.* **285,** 11476–11488 (2010).
117. Kim, D.-H. *et al.* mTOR interacts with raptor to form a nutrient-sensitive complex that signals to the cell growth machinery. *Cell* **110,** 163–75 (2002).
118. Cermak, T. *et al.* Efficient design and assembly of custom TALEN and other TAL effector-based constructs for DNA targeting. *Nucleic Acids Res.* **39,** e82–e82 (2011).
119. Rahrmann, E. P. *et al.* Forward genetic screen for malignant peripheral nerve sheath tumor formation identifies new genes and pathways driving tumorigenesis. *Nat. Genet.* **45,** 756–766 (2013).